The University of South Bohemia in České Budějovice
Faculty of Science

Ageing-associated changes in the expression of epigenetic factors and their impact on longevity in mammals

Bachelor thesis

Vilja Langer

Advisor: Gahurová Lenka, Mgr. Ph.D.

České Budějovice 2024

Langer, V., 2024: Ageing-associated changes in the expression of epigenetic factors and their impact on longevity in mammals. Bc. Thesis, in English – 47 p., Faculty of Science, University of South Bohemia, České Budějovice, Czech Republic.

Annotation

This thesis explores the epigenetic mechanisms potentially influencing ageing and longevity by analysing gene expression levels in kidney and liver tissues of mammals with varying life spans. This study builds on previous bioinformatics research, which established a correlation between epigenetic gene expression and age across species with different life spans, with the primary goal of validating these findings. The obtained results emphasise the possible link between epigenetic modifications and ageing processes using techniques such as RNA extraction, cDNA synthesis, and quantitative PCR. This work underscores the need for further research to understand how these genetic alterations could be targeted to manage age-related conditions and potentially extend life expectancy, thereby contributing to the broader field of genetics research.

Declaration

I declare that I am the author of this qualification thesis and that in writing it I have used the sources and literature displayed in the list of used sources only.

České Budějovice, 07.08.2024

.....

Abstract

Ageing has always been considered a natural, unavoidable, inherent part of life that affects all living organisms. However, epigenetics, a rapidly growing scientific field, has started to uncover the complex regulatory connections that have significant implications for longevity and overall health. This research builds upon previous bioinformatics analyses conducted by our laboratory, which identified specific patterns of epigenetic gene expression levels of fourteen epigenetically relevant genes in kidney and liver tissues correlated with ageing in different mammals with varying life expectancies: short- and long-lived species.

In our current study, we aim to validate these previous findings by experimentally quantifying the expression of relevant genes in the kidney and liver tissues of two short-lived species, mouse and guinea pig. For this purpose, kidney and liver tissues of young and aged individuals were analysed to assess the expression levels of the fourteen genes encoding epigenetic factors. The methodology involved RNA extraction, reverse transcription and quantitative real-time PCR. The gene expression trends observed within our results generally align with the initial bioinformatics data, reinforcing the potential link between epigenetic gene expression and ageing. This sets an initiative for further exploration, looking into how these epigenetic modifications impact longevity and the ageing process in various organisms, potentially leading to advances in managing and treating age-linked conditions. Future studies may also investigate the potential targeting of these epigenetic markers to extend lifespan and promote healthy ageing.

List of abbreviations

5hmC	5-hydroxymethylcytosine
5mC	5-methylcytosine
cDNA	complementary DNA
CpG	5'—Cytosine—phosphate—Guanine—3'
Cq	quantification cycle
Dgcr8	DiGeorge syndrome critical region gene 8
DNMT1	DNA methyltransferase 1
H2a.z	histone 2A variant Z
H3K4me/me2/me3	mono-, di-, trimethylation of histone 3 at lysine 4
H3K9me2/me3	di-, trimethylation of histone 3 at lysine 9
H3K27ac	acetylation of histone 3 at lysine 27
H3K36me3	trimethylation of histone 3 at lysine 36
HP1γ	heterochromatin protein 1γ
Irf7	interferon regulatory factor 7
KAP1	KRAB-associated protein 1
Mybl1	MYB proto-oncogene like 1
Ncoa3	Nuclear receptor coactivator 3
Phf19	PHD finger protein 19
piRNA	piwi-interacting RNA
Prmt1	Protein arginine methyltransferase
PTM	post-translational modification
qPCR	quantitative PCR
Rnasel	Ribonuclease L
Setbp1	SET-binding protein 1
Setd1b	SET domain containing 1B
SRA	SET and RING associated
Tdg	thymine DNA glycosylase
Tet3	ten-eleven translocation 3
Tdrd7	Tudor domain 7
Uhrf1	ubiquitin-like with PHD and ring finger domains 1
Ybx1	Y-box binding protein 1

Table of contents

1. Introduction

Ageing is an inevitable part of life, a multifaceted process influenced by both genetic predisposition and environmental factors. This biological phenomenon is characterised by the deterioration of structural integrity, functional capabilities, and the overall vitality of the organism. The process of ageing is accompanied by deleterious molecular alterations and changes at the cellular level (Rodríguez-Rodero et al., 2011). Despite significant research progress, many aspects of how and why organisms age at the molecular, cellular, and systemic levels remain unclear. The underlying mechanisms of the biological ageing process are still not fully understood.

Epigenetics is a relatively new, rapidly expanding key area of research. This field investigates how certain factors can alter the functionality of our genes without modifying the DNA sequence itself (Hillman & Dale, 2018). Epigenetic changes leading to increased or decreased gene expression can affect ageing and the likelihood of developing diseases. As epigenetic factors can be affected by the environment, this highlights the significant impact of our surroundings and lifestyle choices on gene expressions, showing the complex interplay between our genes and environmental factors in determining our health as we age (Sedivy et al., 2008).

1.1 Epigenome of eukaryotes

In eukaryotic cells, the chromosomal DNA is tightly wrapped around basic proteins, called histones. The positive charges on the histone proteins facilitate an attraction with the negatively charged DNA. This electrostatic interaction causes the DNA to wrap around the histone proteins, leading to the formation of nucleosomes, which further condense into chromatin fibres that serve as the basic building units of the chromatin (Mariño-Ramírez et al., 2005). The DNA itself consists of four different types of nucleotide bases: adenine (A), guanine (G), thymine (T), and cytosine (C).

The epigenome landscape is a result of various mechanisms, processes, and substances that can modify the DNA without changing the underlying sequence (Pal & Tyler, 2016). The two primary epigenetic mechanisms include the histone modifications and the DNA methylation of predominantly cytosine bases, both of which can alter the chromatin conformation and, consequently, the accessibility of genes for transcriptional activity (Sweatt, 2013).

1.2 Covalent histone modifications

Chromatin is a fundamental, complex structure of DNA interwind with proteins found in the nucleus of eukaryotic cells. Chromatin dynamics play a vital role in gene expression, primarily by regulating the accessibility of genetic sequences to transcriptional machinery (Lieberman, 2008).

The chromatin structure has two major structural conformations, the euchromatin and the heterochromatin, each showing a distinct and opposing functionality (Huisinga et al., 2006). Euchromatin, characterised by its loosely packed form, promotes and increases the rate of gene expression by enabling access of transcriptional factors to the DNA sequence, facilitating the transcription process that precedes the translation of genetic information into functional proteins. Conversely, the heterochromatin represses gene expression with its tightly packed structure. The condensed nature of this conformation restricts the access of transcriptional machinery to the DNA, thereby inhibiting gene expression (Kiefer, 2007).

The intricate structure of chromatin is crucial in overseeing regulations of various DNA-mediated processes, including gene transcription, DNA replication, and repair of damaged DNA. Central to chromatin organisation are the H2A, H2B, H3 and H4 histone proteins, which are some of the most conserved proteins among eukaryotes (Wolffe & Pruss, 1996). These four distinct histone proteins can interact with DNA and form the structural core of the nucleosome, around which 145-147 DNA base pairs are coiled. Each nucleosome consists of octamers that are two copies of each histone protein, thereby creating the building block for the chromatin (Luger et al., 1997). Covalent modifications of the histone proteins, such as methylation, acetylation, phosphorylation, or ubiquitination, can either tighten or loosen DNA-histone interactions, consequently impacting the chromatin accessibility to transcription factors and various regulatory machinery (Strahl & Allis, 2000).

The dynamic interplay between euchromatin and heterochromatin structural conformations, driven by the reversible covalent modification of the associated histone proteins, is an epigenetic mechanism that has a vital function in the regulation of gene expression and overall cellular function (Sokolova et al., 2023).

1.2.1 Post-translational histone modification

The epigenetic landscape of the genome heavily influences the architecture of eukaryotic chromatin (Brunner et al., 2014). Histone proteins are subjected to extensive covalent post-translational modifications (PTMs), including acetylation, methylation, and phosphorylation,

that occur at specific amino acid residues (Sidoli et al., 2012). The best-studied PTMs are acetylation and methylation (Pagiatakis et al., 2021).

Acetylation induces covalent modifications at the lysine residues within histone tails, neutralising their positive charge, leading to a relaxed chromatin structure and increased DNA accessibility (Pagiatakis et al., 2021). The addition and the removal of an acetyl group from the lysine residue are mediated by two enzyme classes. Histone acetyltransferases facilitate the transfer of the acetyl group onto the ε-amino group of lysine, thereby increasing transcriptional activity. Conversely, histone deacetylases catalyse the elimination of the acetyl groups and thereby decrease transcriptional activity (Papait et al., 2015).

Methylation of histone tails is another vital epigenetic mark that plays a crucial role in transcriptional regulation. Histone methylation occurs on specific amino acid residues, lysine (L) and arginine (R). Arginine can only be monomethylated, whereas lysine undergoes mono-, di-, and trimethylations (Guo, 2012). The position and degree of methylation on these residues have specific implications (Pagiatakis et al., 2021). For example, many modifications on the histone tails are linked to gene suppression: H3K27me3, the trimethylation of H3 at lysine 27 (Bogliotti & Ross, 2012), as are the dimethylation of H3 at lysine 9, referred to as H3K9me2 (Salzberg et al., 2017) and H3K9me3, the trimethylation of the same site (Ninova et al., 2019). Other histone methylations, however, are associated with transcriptionally active chromatin, such as H3K4me3, the trimethylation of the H3 histone at lysine 4 residue (Beacon et al., 2021), H3K36me3, the trimethylation of at the lysine 36 (Xiao et al., 2021) or H3K4me2, the dimethylation of lysine 4 residues (Broberg et al., 2015), all of which are located on the same histone protein.

1.2.2 The histone isoform H2A.Z

The gene *H2a.z*, encoding the histone isoform H2A.Z, was consistently employed as a control gene throughout this study due to its high level of conservation among eukaryotic species. Its primary biological roles include transcriptional regulation (Redon et al., 2002) and contributing to DNA repair mechanisms (Giaimo et al., 2019). H2A.Z undergoes various PTMs, granting it distinct functionalities (Bönisch & Hake, 2012). The H2A.Z-containing nucleosomes undergo transcriptionally activating acetylation and transcriptionally repressing monoubiquitylation. They are present at the heterochromatin-euchromatin boundaries, aiming to prevent the spread of heterochromatin structure (Draker & Cheung, 2009).

1.3 DNA methylation

Methylation is a common but sparse epigenetic modification in mammals that predominantly occurs at specific locations in the genome, known as the CpG sites (Li & Zhang, 2014). These sites are distinct DNA sequences characterised by the presence of a cytosine base, followed by guanine in the 5′ to 3′ direction (Deaton & Bird, 2011).

DNA methylation is a heritable epigenetic modification catalysed by the enzymes DNA methyltransferases. In contrast, demethylases from the ten-eleven translocation (TET) family are catalysing the removal of the methyl groups (Field et al., 2018). Typically, the methylation occurs at the C5 position of the cytosine ring (Jin et al., 2011), yielding 5-methylcytosine (5mC).

DNA methylation at CpG islands of the promoter region, associated with gene silencing, is an essential regulatory mechanism for correct mammalian development and the maintenance of genomic stability (Senner, 2011). In mammals, it is a critical regulatory element of numerous cellular functions, such as maintaining chromosome integrity, regulating gene expression, or inactivating X chromosomes (Robertson, 2005). CpG islands are generally heavily hypomethylated, and methylation of these sequences can induce undesirable gene suppression, which can cause the development of various diseases, for example, cancer (Li & Zhang, 2014).

In addition to methylation at the promoters, DNA can be methylated at the enhancers, another cis-regulatory element of the genome. In the enhancer region, just as in the promoter region, removing 5mC activates gene expression, whereas adding 5mC suppresses it (Domcke et al., 2015). However, methylation levels in the enhancer region exhibit greater variability, indicating their importance in gene regulation (Sharifi-Zarchi et al., 2017). It has been suggested that changes in this methylation landscape, specifically the increased presence of 5-hydroxymethylcytosine (5hmC), an intermediate of the demethylation process (Ito et al., 2011), in this region, could serve as a predictor for various cancer types (Xu & Gao, 2020).

1.4 Epigenetics, ageing and longevity

An increasing number of research studies have conducted general patterns of alterations that occur as organisms age. On a molecular and cellular level, ageing is associated with a global loss of canonical histones (Yi & Kim, 2020) and the overall reduction in DNA methylation across the genome, while specific regions, particularly CpG islands, experience local hypermethylation (Fraga et al., 2007). Loss of heterochromatin is commonly observed in aged cells across different species (Zhang et al., 2020), and a broad depletion of essential histone proteins from the genome has been documented as well (Pal & Tyler, 2016). These changes lead to the disruption of healthy gene expression patterns, which causes genomic instability and eventually culminates in the deterioration of the organism (Mutirangura, 2019). It has been proposed that a stable epigenome, characterised by specific patterns of epigenetic factor activity, is linked to longevity and healthy ageing (Sen et al., 2016).

Building on these fundamentals, previous research has analysed the epigenome and transcriptome landscapes in ageing mice, examining different tissues. For example, it has been shown that the trimethylation mark at lysine 4 of histone 3, H3K4me3, spreads beyond the usual promoter regions in aged mice. Additionally, the acetylation mark at lysine 27 of histone 3, H3K27ac, tends to cluster more at the enhancer regions of the DNA in these mice. Both modifications cause an increase in gene expression by transforming the chromatin into its active conformation (Benayoun et al., 2019). These findings complement the existing knowledge on the DNA methylation clock, which identifies specific CpG sites where methylation levels strongly correlate with the chronological age in humans. The pattern and methylation levels at these sites can help estimate the tissue's biological age by correlating individual methylation patterns. This forms the foundation of the DNA methylation clock, also known as the epigenetic clock. (Horvath, 2013). Another study observed a notable decrease in overall DNA methylation levels as people aged, evidenced by a higher percentage of methylation in young individuals compared to older groups. This study also found that the age-related decrease in DNA methylation was less pronounced in the offspring of centenarians, who exhibited significantly higher levels of global DNA methylation compared to the descendants of parents who did not live to an advanced age (Gentilini et al., 2013). These findings might indicate a correlation between DNA methylation, longevity, and lifespan.

1.5 Preliminary results from our laboratory

Previous bioinformatics research from our laboratory (Müller, 2022), focused on investigating gene expression changes in tissues from young versus aged individuals in both short-lived and long-lived mammalian species. This study has identified fourteen epigenetically relevant genes with distinct expression patterns tied to the lifespan differences across mammalian species. Specifically, in long-lived species, human and naked mole-rat, the study found that four genes - DiGeorge syndrome critical region 8 (*Dgcr8*), SET domain containing 1B (*Setd1b*), thymine DNA glycosylase (*Tdg*) and ten-eleven translocation 3 (*Tet3*) - showed an intriguing pattern of increased gene expression in older individuals compared to younger ones. Conversely, in short-lived species, mouse and rat, the same genes showed decreased expression levels in correlation with ageing. A different group of genes displayed the opposite expression pattern. This includes the genes interferon regulatory factor 7 (*Irf7)*, MYB proto-oncogene like 1 (*Mybl1)*, Nuclear receptor coactivator 3 (*Ncoa3)*, PHD finger protein 19 (*Phf19)*, Protein arginine methyltransferase (*Prmt1)*, Ribonuclease L (*Rnasel),* SET-binding protein 1 *(Setbp1),* Tudor domain-containing protein 7 *(Tdrd7),* ubiquitin-like with PHD and ring finger domains 1 *(Uhrf1),* and Y-box binding protein 1 *(Ybx1)*. In short-lived species of mammals, these genes showed an upregulation of gene expression in aged individuals compared to younger ones. Contrarily, these genes were expressed at lower levels in aged individuals of the long-lived species (human and naked mole-rat) and exhibited higher expression levels in younger ones. This contrasting behaviour suggests that these genes may regulate epigenetic processes and are potentially linked to the development of age-linked diseases. Moreover, these genes might play a crucial role in promoting longevity by maintaining epigenomic stability, enhancing beneficial epigenetic modifications or, vice versa, accelerating ageing in short-lived species due to less favourable epigenetic changes. Exploring these regulatory epigenetic mechanisms can provide valuable insights into how longevity is determined on a molecular level.

1.5.1 Epigenetic genes that are upregulated in long-lived species during ageing

The genes *Dgcr8*, *Setd1b*, *Tdg* and *Tet3* are associated with various regulatory functions within the cell, particularly in the context of ageing and maintaining cellular health.

DGCR8 maintains the heterochromatin structure by binding to the nuclear envelope protein Lamin B1 and various proteins associated with the heterochromatin, such as KAP1 and HP1γ, utilising its distinct motifs at its N-terminus. Elevated levels of DGCR8 mitigate ageing in

human mesenchymal cells and osteoarthritis in mice, suggesting that this gene has the potential to avert premature cellular senescence (Deng et al., 2019).

Setd1b codes for a protein with a *SET* domain that is part of a histone methyltransferase complex component. This complex is responsible for the methylation of histone 3 on lysine 4, H3K4me, and is found at gene promoters, associated with increased transcription and gene expression (Krzyzewska et al., 2019). By upregulating *Setd1b*, the chromatin transforms into a more open and transcriptionally active state, thereby expressing gene senescence and promoting metabolic processes like beta-oxidation (Nacarelli et al., 2022).

TET3 facilitates the oxidation of 5mC into 5hmC, which marks the initial step of the DNA demethylation process (Barker & Tsai, 2017). Additionally, TET3 can further oxidise genomic 5hmC, continuing the demethylation pathway. This dual role of TET3 might be crucial in decreasing genomic 5hmC during ageing because lower TET3 levels were found in older human T cells (Truong et al., 2015). Deletion of TET3, together with TET2, in T cells leads to severe immune dysregulation in adult mice, which indicates that this gene is at least partially responsible for maintaining T cell homeostasis (Lio & Rao, 2019).

Tdg encodes a member of the DNA repair enzyme family (Cortázar et al., 2011), which facilitates the replacement of the modified cytosine with an unmodified one. Its activity leads to DNA demethylation, essential for gene expression regulation during development (Cortellino et al., 2011; Onabote et al., 2022). TDG has also been proposed as a tumour suppressor. Its loss has been linked to a pre-diabetic state in adult male mice, highlighting its importance in metabolic regulation (Hassan et al., 2020).

1.5.2 Epigenetic genes upregulated during ageing in short-lived species

The overexpression of the genes *Irf7, Mybl1, Ncoa3, Phf19, Prmt1, Rnasel, Setbp1, Tdrd7, Uhrf1,* and *Ybx1* has been linked to various ageing-related diseases and epigenetic alterations. For instance, the gene *Irf7* codes for a transcription factor that participates in innate immune responses against viruses (Bińkowski et al., 2022) and contributes to the silencing of transposable elements (Gázquez-Gutiérrez et al., 2021). Upon a viral infection, it gets phosphorylated, causing it to dimerise and undergo nuclear translocation. This process is triggered by innate immune cells with virus-specific substances such as DNA or RNA (Ma et al., 2023). Elevated IRF7 levels, however, disrupt the balance of metabolic functions within cells, disrupting metabolic homeostasis (Nodari et al., 2021), and can even promote cancer as it was found to increase glioma cells' resistance to radiation and their ability to spread (Kim

et al., 2015). Additionally, it has been shown that IRF7 increases in stromal cells of aged mice (Nodari et al., 2021).

Mybl1 encodes a transcription factor that can bind the DNA through a helix-loop-helix-domain. It was found to drive the synthesis of piRNA precursors and mRNAs encoding piRNAs, which is crucial for silencing transposable elements during meiosis (Tan & Wilkinson, 2023). Increased levels of MYBL1 have been found in tumour cells (Guo et al., 2017).

NCOA3 can recruit histone acetyltransferases and arginine methyltransferases through direct interactions (Wu et al., 2012), and has also been proposed as a predictive marker for breast cancer due to showing an elevated expression level in cancer tissues (Zhao et al., 2003).

PHF19 assists in the demethylation of H3K36me3 by binding to it via its Tutor domain and recruiting H3K36 histone demethylases (Ballaré et al., 2012). It has been shown that reduced trimethylation at H3K36 occurs as cells age, leading to hyperacetylation and, consequently, heightened chromatin accessibility (Sen et al., 2015). PHF19 was found to be upregulated in various types of cancer (Ghamlouch et al., 2021).

Prmt1 encodes an enzyme that facilitates the methylation of arginine on different types of proteins, including histones (Zhu et al., 2022). This gene's increased expression is connected to different types of cancer (Musiani et al., 2020).

RNASEL plays a role in suppressing retrotransposition of transposable elements (Zhou et al., 2020), and its activity can lead to cell senescence or programmed cell death. Activating RNASEL through 2-5A transfection leads to prostate cancer cell death and induces ageing in healthy prostate epithelial cells (Andersen et al., 2007), suggesting its potential as a biomarker for prostate cancer due to its elevated levels in these malignant cells (Kocić et al., 2022).

Setbp1 can bind to the promoter region of genomic DNA, initiating gene expression by recruiting epigenetic complexes (Piazza et al., 2018). Its overexpression has been associated with inducing mutations in its expression, ultimately leading to myeloid leukaemia (Linder et al., 2017).

Tdrd7 transcribes a protein that controls post-transcriptional gene expression. It has been shown that this gene plays a significant role in enabling chromatin accessibility in primordial germ cells (Anand et al., 2021; D'Orazio et al., 2021). *Tdrd7* has been linked to the development of glaucoma and cataracts (Anand et al., 2021). Cataract is caused by the age-related breakdown of proteins found in the human lens (Sarkar et al., 2023).

UHRF1 can maintain DNA methylation by serving as a cofactor for DNMT1, a DNA methyltransferase. It has a high affinity for hemimethylated DNA, to which it binds through its SRA domain (Newkirk & An, 2020). UHRF1 targets specific methylated histones, such as H3K9me2/me3, to target them for ubiquitination, which facilitates the methylation process by recruiting DNMT1. (Vaughan et al., 2019). It promotes gastric cancer growth by the excessive methylation of the genes that typically suppress the tumours (Zhou et al., 2015), and it also facilitates oncogenic pathways in lung cells (Kostyrko et al., 2023).

Ybx1 encodes a transcriptional regulator protein belonging to the Cold Shock Domain family (Kuwano et al., 2019) that can bind to the Y-box of the DNA, found in the promoter and enhancer regions of many genes. It affects various cell processes, such as splicing and translation, and functions as an RNA-binding partner. (Dinh et al., 2024). YBX1 has been associated with various types of cancer, such as lung adenocarcinoma (Xie et al., 2021), breast cancer (Lim et al., 2017)

2. Aims

The aims of this research are:

I. to compare the changes in expression levels of selected epigenetic factors between young and aged individuals in two short-lived mammalian species

II. to verify the reproducibility of bioinformatics discoveries in our laboratory through experimental measurement of the analysed genes

This study seeks to explore a possible link between lifespan and epigenetic markers in mammals by validating the bioinformatics research of our laboratory (Müller, 2022), which identified distinctive patterns of gene expression linked to ageing and the overall lifespan. Beyond establishing a potential relationship between mammalian longevity and epigenetic stability, the outcomes of this study could further enhance our understanding of the mechanisms underlying healthy ageing so that targeted intervention to stabilise the epigenome might be able to help mitigate the natural process of physiological decline.

3. Materials and methods

For the experimental quantification of the fourteen epigenetically relevant genes, the sample tissues were collected from two short-lived mammalian species, the mouse (*Mus musculus*) and the guinea pig (*Cavia porcellus*).

3.1 Sample tissue collection

The sample tissues were systematically extracted from the organs consistent with those analysed in the bioinformatic research (Müller, 2022), specifically the liver and kidney. For each of the species being studied, tissues were collected from four aged and at least two young females. The age of young individuals was eight weeks for mouse and three months for guinea pig, whereas the age of aged individuals was 18 months for both mouse and guinea pig. While the sex of the animals was not a determining factor for this study, the selection of females was exclusively to accommodate the requirements of other laboratory studies. To mitigate the risk of contamination, the workspace and all the employed instruments were sterilised prior with ethanol. Subsequently, the freshly collected tissue samples were immediately immersed in liquid nitrogen to preserve the cellular integrity and avoid RNA degradation and were stored at a temperature of -80°C until further processing.

3.2 RNA extraction

The RNA was isolated following the TRIzol™ Reagent (Ambion). At first, the samples kept at a freezing temperature of -80 °C were thawed on ice. Following the initial cell lysis and the homogenisation with TRIzol™ (1 mL per ~100 mg of tissue), the sample was incubated at room temperature for five minutes. A centrifugation step at full speed for three minutes at room temperature followed, after which the upper aqueous supernatant that contains the RNA was carefully pipetted into a new Eppendorf tube. The RNA extraction continued through a liquid-liquid phase separation achieved by adding 0.2 mL chloroform to the mixture. The solution was stirred vigorously and incubated for two minutes at room temperature. Following another centrifugation step at full speed for fifteen minutes at 4 °C, RNA pellet precipitation from the aqueous phase was initiated by adding 2 µL of 20 mg/mL glycogen (ThermoFisher Scientific) and 0.5 mL of 100% isopropanol. The mixture was incubated for ten minutes at room temperature and was then centrifugated at full speed for 20 minutes at 4 °C. The supernatant was disposed of, and the RNA pellets were washed with 1 mL of 75% ethanol. Subsequently, the wash was discarded after a centrifugation step at full speed for 8

minutes at 4 °C. The pellets were air-dried for 5-10 minutes and resuspended in 20-40 µL of RNase-free water, depending on the size of the pellet. The extracted RNA was washed with 1 mL 75% ethanol; the wash was discarded after a centrifugation step at full speed for eight minutes at 4 °C. The pellets were air-dried for five to ten minutes before being resuspended in 20-40 µL of RNase-free water; the added volume was contingent on the size of the pellet. The purity of RNA was assessed with a NanoDrop spectrophotometer. This involved measuring the absorbance ratios of 280/260 to determine purity and the 260/230 absorbance ratios to evaluate the presence of possible organic molecule contamination.

3.3 DNase treatment

The purified RNA was treated with TURBO DNA-free™ (Ambion) to remove potential genomic DNA contamination. For this purpose, 2.4 µL of the TURBO™ DNase enzyme and 4.8 µL of the 10x TURBO™ DNase buffer were added to each of the RNA samples resuspended with water to a volume of 40 µL. To adjust for the smaller sample suspension volumes, the quantities of the reagents were proportionally reduced. The reaction mixture was incubated in a thermoblock at 37 °C for 30 minutes. To quench the reaction, 9.6 µL of DNase Inactivation Reagent was added. After centrifugation at full speed for two minutes at room temperature, the supernatant containing the DNA-free RNA was extracted for further processing.

3.4 Reverse transcription

The complementary DNA (cDNA) was synthesised in accordance with the Thermo Scientific™ RevertAid reverse transcription protocol. The initial reaction mixture was prepared by combining 4.0 µL of the purified RNA sample with 1.6 µL of the 50 µM Oligo d(T)16 primers and with 3.0 µL of RNase-free water. The mixture was heated in a thermocycler for five minutes at 70 °C, then cooled at 4 °C for ten minutes. Next, 3.9 µL RNase-free water, 4.0 µL of the 5x Reaction buffer, 2.0 µL 10mM deoxynucleotide triphosphate (dNTP), 0.5 µL of Riboblock, 1.0 µL RevertAid H Minus Reverse Transcriptase were added. The mixture was placed in the thermocycler with a pre-programmed reverse transcription cycle of five stages: ten minutes at 25 °C, five minutes at 37 °C, seventy-five minutes at 42 °C, ten minutes at 70 °C, and cooling phase down to 4 °C. The synthesised cDNA was checked for purity and contamination using the NanoDrop spectrophotometer. The absorbance ratios of 280/260 and 260/230 were checked to confirm purity and the absence of organic contaminants.

3.5 Analysis with quantitative real-time PCR (qPCR)

The expression levels of the fourteen epigenetic markers were quantitively assessed using the CFX Opus Real-Time PCR System. The primers for qPCR had been previously designed to either anneal to exon-exon junctions or to span intronic sequences to prevent any potential amplification of any remaining genomic DNA. The primers were designed in a way that they had identical, or at least highly similar nucleotide sequences for the same gene across the different species (*Table 1)*, thereby maximising the consistency of the double-stranded DNA products across species, which was generated by qPCR. Primer sequences were designed using Primer3web v4.1.0 tool (https://primer3.ut.ee/).

Every measurement was conducted in 98-well plates, separating samples based on age, species, and organs. The analysis was executed in triplicates to ensure the reliability of the measured expression for each gene of interest. Each qPCR assay contained 1 µL of the cDNA sample (50-300 ng) and 9 µL of a master mix containing 5µL 2x SYBR™ Green (ThermoFisher Scientific), 0.3 µL 10µM forward primer, 0.3 µL 10µM reverse primer and 3.4 µL RNase-free water. The negative control was run with the same reagent mixture but with 1 µL of RNase-free water instead of cDNA.

The qPCR was performed using SYBR Green as the fluorescent dye to monitor the amplification process. The protocol began with the initial denaturation step, conducted at 95 °C for 15 minutes, followed by 40 cycles of amplification. Each cycle consisted of denaturation at 94 °C for 25 seconds, primer annealing at 57 °C for 25 seconds, and elongation at 72 °C for 30 seconds. The cycle threshold (Ct) was recorded to note the number of necessary amplification cycles for the fluorescence intensity to surpass the predefined threshold limit. Relative gene expression levels across the different age groups were estimated by the delta-delta Cq method, with *H2a.z* as a reference gene commonly used in the laboratory.

3.5.1 The delta-delta Cq method

Each sample was measured in triplicates, and the averages of the quantification cycles (Cq) values were determined as shown in *Equation 1* for further calculation steps.

$$Cq_{avg}(\text{gene}) = (Cq_1 + Cq_2 + Cq_3) / 3 \quad (1)$$

The housekeeping gene *H2a.z* was measured individually in the same qPCR run for each sample to serve as a normalisation factor. This standardisation step was necessary to mitigate inconsistencies within the qPCR runs. For this purpose, the ΔCq values were calculated, as specified in *Equation 2.*

$$\Delta Cq = Cq_{avg}(\text{target gene}) - Cq_{avg}(H2a.z) \quad (2)$$

The arithmetic mean of ΔCq was calculated from samples of younger individuals, and this value was subtracted from each ΔCq value of the aged subjects, as shown in *Equation 3*.

$$\Delta\Delta Cq = \Delta Cq \text{ (aged)} - \Delta Cq_{avg} \text{ (young)} \quad (3)$$

The relative expression levels of the target gene in aged specimens, compared to the young ones, were determined with *Equation 4*.

$$\text{fold change} = 2^{(-\Delta\Delta Cq)} \quad (4)$$

Fundamentally, lower Cq values indicate a greater initial concentration of the target gene as it reached the Ct value in fewer cycles. Subsequently, negative ΔΔCq values suggest increased gene expression levels in aged individuals when compared to younger ones, and positive ΔΔCq suggest the opposite. The fold change incorporates the characteristic exponential growth phase of the polymerase chain reaction (PCR).

Table 1 - Nucleotide sequences of the primers used in qPCR

H2a.z (control gene)	guinea pig	forward	5'- CAAGGCCAAGACAAAGGGTG -3'
		reverse	5'- GCCAGTTCAAGCACCTCTG -3'
	mouse	forward	5'- GCGCAGCCATCCTGGAGTA -3'
		reverse	5'- CCGATCAGCGATTTGTGGA -3'
Dgcr8	guinea pig	forward	5'-CGCGGGTGGTGTAAGAATAA-3'
		reverse	5'-TGTTTAACCATTTTACTGCT-3'
	mouse	forward	5'-CGCGGGTGGTGTAAGAATAA-3'
		reverse	5'-TGTTGACCATTTTGCTGCT -3'
Irf7	guinea pig	forward	5'-TGCGGTTCGGAGAGTGGCTA-3'
		reverse	5'-GCAAATGCTTCCAGGGTACG-3'
	mouse	forward	5'-TGCTGTTTGGAGACTGGCTA -3'
		reverse	5'-GCAAATGCTTCCAGGGTACG-3'
Mybl1	guinea pig	forward	5'-TGGGCAGAAATTGCCAAACTA-3'
		reverse	5'-AGCCCTCCTGTTCCACTTTT-3'
	mouse	forward	5'-TGGGCCGAGATTGCTAAGTTA-3'
		reverse	5'-AGCCCTCCTGTTCCACTTTT-3'
Ncoa3	guinea pig	forward	5'- ACAGTAAGACAGATACGTCA -3'
		reverse	5'- CTCCTTGTCCTGTAGAAGAT -3'
	mouse	forward	5'- ACAGTGAGACAGATACGGCA -3'
		reverse	5'- CTCCCTGCCCTGTAGAAGAC -3'
Phf19	guinea pig	forward	5'- TCCTCAACGCCCTCAACAGC -3'
		reverse	5'- TTCTCACTCAGTACCAGACC -3'
	mouse	forward	5'- TCCTCAACGCTCTCAACAGT-3'
		reverse	5'- TTGTCACTTGGCATCAACGC-3'

Prmt1	guinea pig	forward	5'- GCCTGCAAGTGAAGCGGAAC -3'
		reverse	5'- GATCTCCTCGCCCGTCTTCA -3'
	mouse	forward	5'- GCCTGCAAGTGAAGAGGAAC -3'
		reverse	5'- GATCTCCTCGCCAGTCTTCA -3'
Rnasel	guinea pig	*Rnasel* is not annotated	
	mouse	forward	5'- GGACCTCATTCATTGCCTGT -3'
		reverse	5'- CCGGAGTGTTCTATAGCGGT -3'
Setbp1	guinea pig	forward	5'- CTGGGGACCAGAAAGTGTCC -3'
		reverse	5'- CCTCTCATAAGCCTGTGGCT -3'
	mouse	forward	5'- CTGCCCACCTGAGATCAAGA -3'
		reverse	5'- CCTCTCGTATGCCTGTGTCT -3'
Setd1b	guinea pig	forward	5'- AAGGTCAAGAGGAAGGAGCC -3'
		reverse	5'- TCCCGCTCGGACTCTTCATC -3'
	mouse	forward	5'- AAGGTCAAGAGGAAGGAGCC -3'
		reverse	5'- TCCCGCTCTGACTCTTCATC -3'
Tdrd7	guinea pig	forward	5'- CGTCTGTATTGGTGGTTGAA -3'
		reverse	5'- GGTGCAGCCATGGAGTTCTT -3'
	mouse	forward	5'- CGTCTGTGTTGGTGGTTGAG -3'
		reverse	5'- AAGACTCCTGTACTGCCACC -3'
Tdg	guinea pig	forward	5'- TCCTGACCTGGCAGCCCCGG -3'
		reverse	5'- GACGCCCTGGCTTTCCTTTT -3'
	mouse	forward	5'- TCCTAACATGGCAGTCACGA -3'
		reverse	5'- GCTGCTCTGGGTTTCCTTTT -3'
Tet3	guinea pig	forward	5'- TTCCCCACTTGCGATTGTGT -3'
		reverse	5'- GGAGCTCTTCCCCTCCTTCC -3'
	mouse	forward	5'- TTCCCTACCTGCGATTGTGT -3'
		reverse	5'- AGAACTCTTCCCCTCCTTGC -3'
Uhrf1	guinea pig	forward	5'- CGTGGACTCGCTGTCCAGGT -3'
		reverse	5'- TGGCCATCCTCCATCTGCTT -3'
	mouse	forward	5'- CGTGAACTCTCTGTCCAGGT -3'
		reverse	5'- TGGCCATCCTCCATCTGTTT -3'
Ybx1	guinea pig	forward	5'- GAGAAGTGATGGAGGGTGCT -3'
		reverse	5'- GGCCCCTGCGGAATCGTGGT -3'
	mouse	forward	5'- GAGAAGTGATGGAGGGTGCT -3'
		reverse	5'- GGCCCCTGAAATGAATGCTT -3'

3.6 Data evaluation

The fold change values, determined from the qPCR quantification cycles, were processed by transforming them using base 2 logarithms and calculating their averages. Negative values within the transformed data indicate downregulation, while positive ones indicate upregulation. To showcase a variation among samples of young individuals, the difference in individual ΔCq values compared to the average ΔCq_{avg} of the young samples was also calculated. Standard deviations for each dataset were computed as well.

Additionally, the Mann-Whitney U test was employed to assess whether there is a significant difference in gene expression levels between the two target age groups. This involves comparing the ΔCq values of young individuals against the ΔCq values of aged individuals, seeking to find significant variations. The statistical analysis was conducted in the R programming language, aiming for a significance level of $\alpha = 0.05$.

4. Results

To verify the bioinformatics results using qPCR, RNA was extracted from the kidney and liver tissues of young and aged mouse and guinea pig females. Its quality was measured before proceeding to synthesise cDNA by reverse transcription. To ensure the reliability of the results, the quality of cDNA was assessed and used for subsequent qPCR runs. The housekeeping gene *H2a.z* was included in all the qPCR assays to quantify relative expression values. The obtained data were statistically analysed to validate the gene expression levels observed in the bioinformatics research.

4.1 Mouse

For the quantification analysis of gene expression in liver and kidney tissues, eight female mice were used: four young (YM-1 to YM-4) and four aged (AM-1 to AM-4).

4.1.1 Absorbance ratios

The absorbance ratios to assess the purity of the samples were measured for all the samples except the RNA of aged mice kidneys and the liver RNA sample of a young mouse number 3 (YM-3). A ratio of approximately 2.0 at 260/280 nm is generally considered an indication of high-purity RNA with minimal contamination. For cDNA, this value lies at approximately 1.8. Typically, the desired 260/230 ratio ranges between 2.0 and 2.2 to ensure the absence of contaminants.

Based on the absorbance measurement results presented in *Table 2*, the absorbance ratios for both RNA and cDNA in liver and kidney tissues generally approach the ideal benchmark values, although some ratios are slightly lower than optimal. Considering that most absorbance ratios are close to the ideal values, we proceeded with these samples for further analysis.

Table 2 - Absorbance measurements of mouse RNA and cDNA

	Kidney				**Liver**			
	RNA		**cDNA**		**RNA**		**cDNA**	
	260/280	**260/230**	**260/280**	**260/230**	**260/280**	**260/230**	**260/280**	**260/230**
AM-1	-	-	1.97	1.88	2.23	2.23	2.23	2.23
AM-2	-	-	1.81	1.89	2.24	2.24	2.24	2.24
AM-3	-	-	1.98	1.74	1.83	1.83	1.83	1.83
AM-4	-	-	1.91	1.71	2.03	2.03	2.03	2.03
YM-1	2.13	1.91	1.94	1.72	1.89	1.89	1.89	1.89
YM-2	2.38	1.87	1.86	1.72	1.84	1.84	1.84	1.84
YM-3	2.24	2.03	2.21	1.88	-	-	-	-
YM-4	2.41	2.28	2.31	1.69	1.89	1.89	1.89	1.89

4.1.2 Mouse kidney

Figure 1 illustrates the log2 fold changes in the kidney tissue of aged mice, from which it can be seen that among all the tested genes, *Tet3, Tdg,* and *Setd1b* demonstrate a general pattern of decreased gene expression in aged mice; however, *Setd1b* does show a minor upregulation in one of the kidney samples. The most pronounced downregulation is found in *Tet3,* with an average log2 fold change of -2.08. *Tdg* exhibits the most consistent pattern of downregulation, whereas *Setd1b* exhibits the highest variation among the downregulated genes. Meanwhile, two genes, *Setbp1* and *Prmt1*, have stable gene expression levels across both age groups, supported by minimal upregulation.

From the upregulated genes, *Rnasel* shows the most profound upregulation in aged mice, with an average of 7.08 and a minimal standard deviation. *Ncoa3* and *Phrf19* also display a notable increase in expression levels in aged samples, with averages of 4.61 and 4.41, respectively. However, both genes have considerable deviation ranges. *Irf7* and *Tdrd7* also display notable upregulation with averages of 3.23 and 2.04, with *Tdrd7* being more consistently overexpressed. *Mybl1* show a variable increase in gene expression with an average log2 fold change of 2.82. The expression levels of *Uhrf1* are moderately higher in aged samples, though this upregulation varies widely. *Ybx1* demonstrates a consistent moderate increase, while *Dgcr8* exhibits mild, consistent upregulation with an average of 0.97.

In young mouse kidneys, the standard deviations of gene expression levels are the most consistent in the genes *Tdg*, *Mybl1*, *Setd1b*, *Tet3* and *Tdrd7.* The genes *Prmt1*, *Uhrf1, Dgcr8, Ybx1, Setbp1, Irf7* and *Rnasel* vary moderately. The highest variability among the kidney samples of young individuals is found in the genes *Ncoa3* and *Phrf19*.

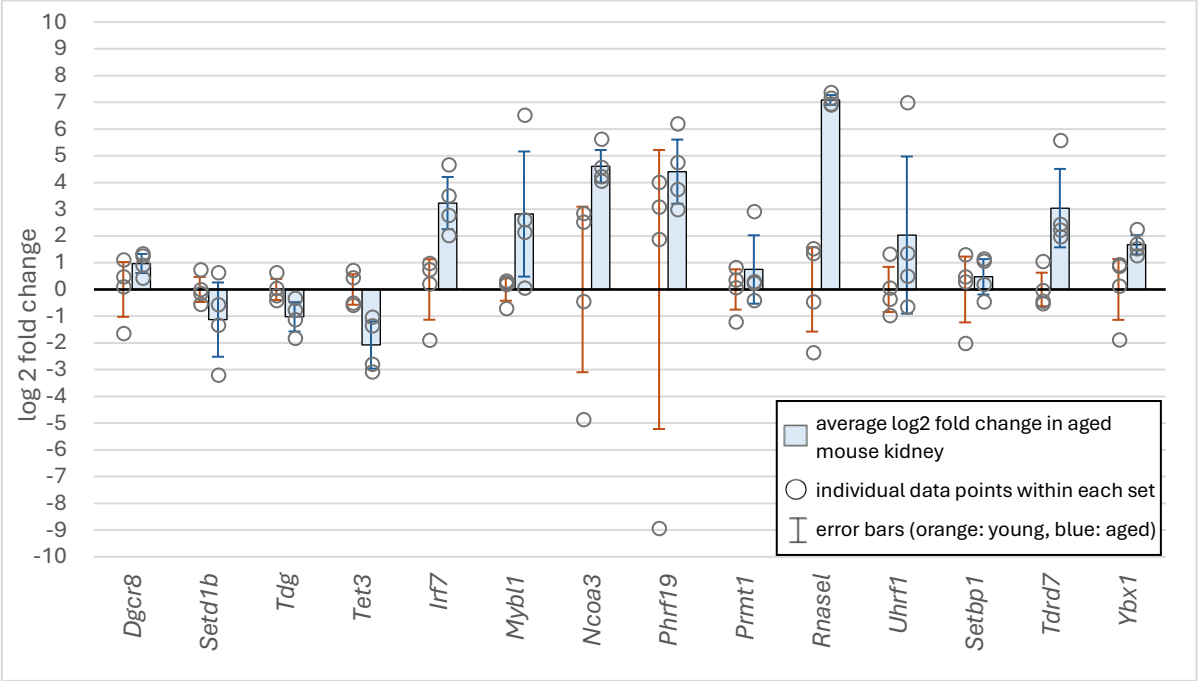

Figure 1 – Gene expression variability in mouse kidney. Blue error bars represent the standard deviation of the log2 fold change in aged to young. Orange error bars show the standard deviation within young individuals.

The statistical analysis to determine whether specific genes exhibit significant changes in expression levels between aged and young mice found that the expression level of *Tet3* is significantly reduced in aged mice. *Irf7* and *Rnasel* show a significant increase in expression levels in aged mice. Derived from the Mann-Whitney U test, these three genes have p-values of approximately 0.03, below the 0.05 significance threshold (*Table 3*). Despite finding no significant difference compared to young samples in the following genes, *Tdg*, *Ncoa3, Mybl1, Tdrd7*, and *Ybx1* demonstrate exclusively an increase or a decrease in gene expression levels in aged mice. From these, *Tdg* and *Mybl1* have p-values of 0.06, slightly above the threshold.

Table 3 - Quantification cycle differences in mouse kidneys and the p-values for statistical significance

KIDNEY	**ΔCq** (young)				**ΔCq** (aged)				
	YM-1	**YM-2**	**YM-3**	**YM-4**	**AM-1**	**AM-2**	**AM-3**	**AM-4**	**p-value**
Dgcr8	6.27	6.64	7.28	4.52	4.85	5.28	5.76	4.93	0.34
Setd1b	6.14	7.03	6.28	5.74	5.68	6.88	7.65	9.50	0.49
Tdg	5.17	6.03	5.44	4.98	5.74	6.18	6.54	7.24	0.06
Tet3	5.92	6.87	7.14	5.84	9.25	7.49	7.82	9.53	0.03
Irf7	8.36	9.13	8.89	6.26	3.50	5.40	6.15	4.66	0.03
Mybl1	8.72	8.80	8.66	7.76	8.44	5.89	1.97	6.36	0.06
Ncoa3	9.79	13.08	12.76	5.37	6.21	4.64	5.69	6.04	0.20
Phrf19	17.10	18.31	19.22	6.28	10.49	11.50	12.25	9.05	0.34

Prmt1	5.16	4.68	4.40	3.13	4.12	4.06	1.43	4.77	0.49
Rnasel	12.25	14.06	14.23	10.34	5.57	5.83	5.36	5.79	0.03
Uhrf1	7.90	9.60	8.32	7.29	8.93	6.94	1.30	7.79	0.34
Setbp1	6.68	6.87	7.70	4.39	6.89	5.36	5.28	6.23	0.69
Tdrd7	6.70	7.09	8.19	6.61	4.94	5.18	1.58	4.72	0.20
Ybx1	5.21	5.95	6.02	3.21	3.85	3.58	2.86	3.41	0.11

Although most of the differences in expression levels in the mouse kidneys between the two age groups are not statistically significant, the observed trends largely match the predictions of the bioinformatics research, in which four genes - *Dgcr8, Tdg, Tet3* and *Setd1b* - showed a consistent pattern of downregulation. In contrast, the other ten genes exhibited steady upregulation in aged short-lived species compared to younger ones. This is supported by the downregulation of the genes *Tdg, Tet3*, and *Setd1b* with average log2 fold changes ranging from -1.13 to -2.08, and the upregulation of the genes Irf*7, Mybl1, Ncoa3, Phrf19, Rnasel, Uhrf1, Tdrd7* and *Ybx1* with average log2 fold changes ranging from 1.67 and 7.08, with *Ybx1* experiencing the smallest increase in upregulation and *Rnasel* displaying the most substantial rise. This increase in gene expression of *Rnasel* was found to be statistically significant, with *Tet3* being the only other gene within kidney samples that delivered statistically significant differences between the two aged groups. Both genes recorded a p-value of 0.03, below the 0.05 significance threshold.

One exception that did not align with the predictions is the gene *Dgcr8.* It was bioinformatically predicted to be downregulated during ageing, while the laboratory results showed its slight upregulation in the kidney tissues of aged mice with an average log2 fold change of 0.97. This upregulation, however, is quite weak, such as the upregulation of the genes *Setbp1* and *Prmt1*, which show average log2 fold changes of 0.47 and 0.75, respectively. These might indicate that their expression levels stay relatively constant throughout the lives of mice instead of being upregulated.

4.1.3 Mouse liver

The log2 fold changes within the liver tissue in aged mice are presented in *Figure 2*. Of the 14 genes displayed, *Tdg* is the only one downregulated, with an average log2 fold change of -2.19. Meanwhile, *Prmt1* is the only gene consistently expressed in young and aged individuals with an average log2 fold change of -0.20; however, it also displays the second largest variability between the two age groups, surpassed only by *Setd1b*.

Within the upregulated genes, *Phrf19* and *Uhrf1* have the highest positive log2 fold changes, with both having a log2 fold change average close to 4.5. However, the deviation range of *Uhrf1* is higher than that of *Phrf19*. *Mybl1* and *Ncoa3* demonstrate a notable upregulation, with an average of 4.03 and 3.92, respectively. However, the standard deviation of *Ncoa3* is significantly lower than that of *Mybl1*. The genes *Setbp1*, *Irf7, Tet3, Rnasel, Tdrd7,* and *Dgcr8* all demonstrate a moderate increase in gene expression among aged individuals, with average log2 fold changes ranging from 1.73 to 2.71. These genes exhibit a clear trend of upregulation, however, with varying standard deviations. For instance, *Irf7, Tet3, Rnasel,* and *Setbp1* all have standard deviations exceeding one, contrasting with the lower variability observed in *Dgcr8* and *Tdrd7*. Meanwhile, *Setd1b* and *Ybx1* show moderate gene upregulation with average log2 fold changes of 1.13 and 0.92, respectively.

In young mouse livers, the standard deviations are the most consistent in the genes *Irf7*, *Phrf19*, *Dgcr8* and *Setbp1.* The genes *Tet3*, *Prmt*, *Ybx1, Mybl1*, and *Tdrd7* exhibit a moderate deviation. In contrast, *Rnasel, Ncoa3, Uhrf1* and *Tdg* display a significant variability, with *Setd1b* showing the highest spread among all tested genes within liver samples of young individuals.

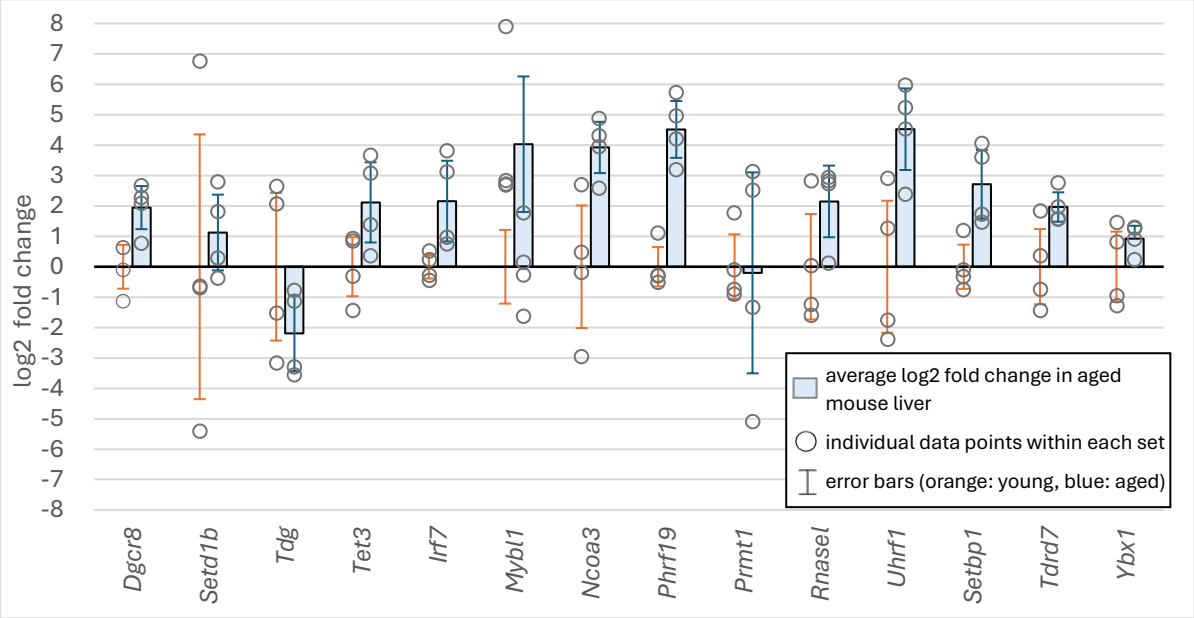

Figure 2 – Gene expression variability in mouse liver. Blue error bars represent the standard deviation of the log2 fold change in aged to young. Orange error bars show the standard deviation within young individuals.

The assessment to determine whether some genes significantly differ in expression levels between aged and young mice revealed that *Irf7, Mybl1, Phrf19, Setbp1,* and *Tdrd7* expression levels show a statistically significant increase in aged mice. These five genes each have p-values of around 0.03, derived from the Mann-Whitney U test, falling below the 0.05 significance level results (*Table 4*). Although the remaining genes do not meet the statistical significance level, many other genes such as *Dgcr8, Tdg, Tet3, Ncoa3, Rnasel, Uhrf1,* and *Ybx1,* demonstrate a distinct pattern of either exclusive upregulation or downregulation in aged individuals. The genes *Dgcr8*, *Ncoa3,* and *Uhrf1* have the lowest p-values (0.06), which lie close to the significance level.

Table 4 - Quantification cycle differences in mice livers and the p-values for statistical significance

LIVER	**ΔCq (**young**)**				**ΔCq (**aged**)**				
	YM-1	**YM-2**	**YM-3**	**YM-4**	**AM-1**	**AM-2**	**AM-3**	**AM-4**	**p-value**
Dgcr8	7.74	5.99	7.01	7.76	5.04	4.86	4.47	6.36	0.06
Setd1b	2.40	7.17	7.12	14.57	6.00	5.03	8.20	7.53	> 0.99
Tdg	0.58	6.74	6.15	2.56	5.23	4.87	7.65	7.38	0.34
Tet3	10.70	8.16	9.30	10.54	6.54	5.95	9.26	8.23	0.11
Irf7	5.07	4.11	4.79	4.28	0.75	1.44	3.81	3.60	0.03
Mybl1	8.90	10.67	10.25	12.29	7.81	7.70	7.84	2.64	0.03
Ncoa3	7.40	8.07	10.28	4.63	2.73	3.30	5.02	3.65	0.06
Phrf19	10.41	10.62	12.03	10.64	5.20	6.73	7.73	5.97	0.03
Prmt1	6.83	6.19	6.03	8.71	4.43	3.82	12.04	8.28	0.89
Rnasel	6.03	7.31	10.09	5.68	7.17	4.34	4.46	4.55	0.11
Uhrf1	13.97	8.67	9.30	12.32	6.54	5.84	8.69	5.09	0.06
Setbp1	9.15	10.44	8.49	8.92	5.20	5.65	7.52	7.79	0.03
Tdrd7	5.41	6.52	4.72	7.99	4.60	3.40	4.19	4.58	0.03
Ybx1	4.37	6.47	4.70	7.11	4.37	4.76	5.43	4.40	0.20

The trend observed in gene expression quantification in mouse liver largely correlated with those found in the bioinformatics research, though most of these differences were not statistically significant. The genes that behaved differently than expected are *Dgcr8, Tet3, Setd1b* and *Prmt1*, from which the first three were downregulated in the bioinformatics results as opposed to upregulated in the experimental findings. Meanwhile, *Prmt1* showed almost no difference between aged and young mouse liver tissues, primarily due to its high variability and statistically insignificant results. Nevertheless, this trend contrasts with the previous findings, which found it to have higher expression in aged short-lived species.

In comparing kidney and liver tissues from mice, the experimental results suggest similar gene behaviour across both organs, with a few notable differences. Three genes exhibited a different expression pattern within the two organs: *Tet3* and *Setd1b* were downregulated in aged mouse kidney tissues and upregulated in their livers. *Setbp1* shows a consistent gene expression pattern between the two age groups in the kidney samples and is upregulated in aged mouse liver. While only a few results are statistically significant, they provide insight into the overall gene expression trend across the different tissues and age groups.

4.2 Guinea pig

For the quantification analysis of gene expression in liver and kidney tissues, six female guinea pigs were utilised: two young (YGP-1, YGP-2) and four aged (AGP-1 to AGP-4). This analysis, however, did not include the *Rnasel* gene as this is not annotated in guinea pigs.

4.2.1 Absorbance ratios

The absorbance ratios at 268/280 and 260/230 were measured for all the cDNA samples of young and aged guinea pigs. The measured absorbance ratios shown in *Table 5* indicate a high purity of the cDNA samples, as most 260/280 ratios are around 1.8, with a few samples having only a slightly higher value. The obtained ratios for 260/230 lie within the interval of 2.0 - 2.2 or just slightly below the ideal reference point. Even though the RNA quality was not directly assessed for the guinea pig samples, the cDNA samples were deemed good quality based on the obtained absorbance ratios. The relatively high purity of the cDNA, which had been synthesised from RNA, implies that the original RNA also had to be relatively pure. For these reasons, the cDNA samples were confidently used for further analysis.

Table 5 - Absorbance ratios of the guinea pig cDNA samples

cDNA	**YGP-1**	**YGP-2**	**AGP-1**	**AGP-2**	**AGP-3**	**AGP-4**
	Kidney					
260/280	1.81	1.79	1.84	1.87	2.06	2.03
260/230	2.01	2.17	2.05	2.01	2.13	2.22
	Liver					
260/280	1.86	1.93	1.82	1.87	1.89	1.91
260/230	1.93	2.05	2.11	2.17	1.94	2.06

4.2.2 Guinea pig kidney

The log2 fold changes in the kidney tissues of aged guinea pigs are demonstrated in *Figure 3*. The genes *Tet3, Tdg, Setd1b* and *Tdrd7* demonstrate a consistent pattern of decreased gene expression in the kidney tissues of aged guinea pigs. The most significant decrease was found in *Setd1b,* followed by *Tdg,* with average log2 fold changes of -4.89 and -3.30, respectively. Each kidney sample supports this trend of downregulation, although the quantification of *Tdrd7* was unsuccessful in one of the aged guinea pig samples.

The genes *Mybl1* and *Uhrf1* show a slight upregulation in the kidneys of aged guinea pigs, although the gene quantification for *Mybl1* did not work in one of the aged samples. The genes *Dgcr8, Irf7, Phrf19, Prmt1, Setdbp1* and *Ybx1* are found to have a profound increase in expression levels in aged guinea pig kidney samples, as their average log2 fold change values range from 2.71 to 6.28 with *Irf7* being the most drastically upregulated and coincidently having the highest variation in expression levels. The quantification of *Dgcr8* was unsuccessful in two aged guinea pig samples despite displaying the most consistent upregulation with the lowest variability.

The quantification of expression levels of the gene *Ncoa3* did not deliver presentable results, as the number of cycles required exceeded the threshold benchmark of the qPCR during every attempt in the young guinea pig samples. Therefore, it was not possible to determine the average log2 fold change, so this gene is categorised as not assessed (N/A) for the guinea pig kidney.

In young guinea pig kidneys, the standard deviations of gene expression levels are the most consistent in the genes *Dgcr8, Tdg, Irf7* and *Phrf19,* with *Dgcr8* having the lowest value of 0.11. The highest standard deviations are found in the genes *Setbp1, Prmt1* and *Tdrd7,* ranging from 1.66 to 3.51.

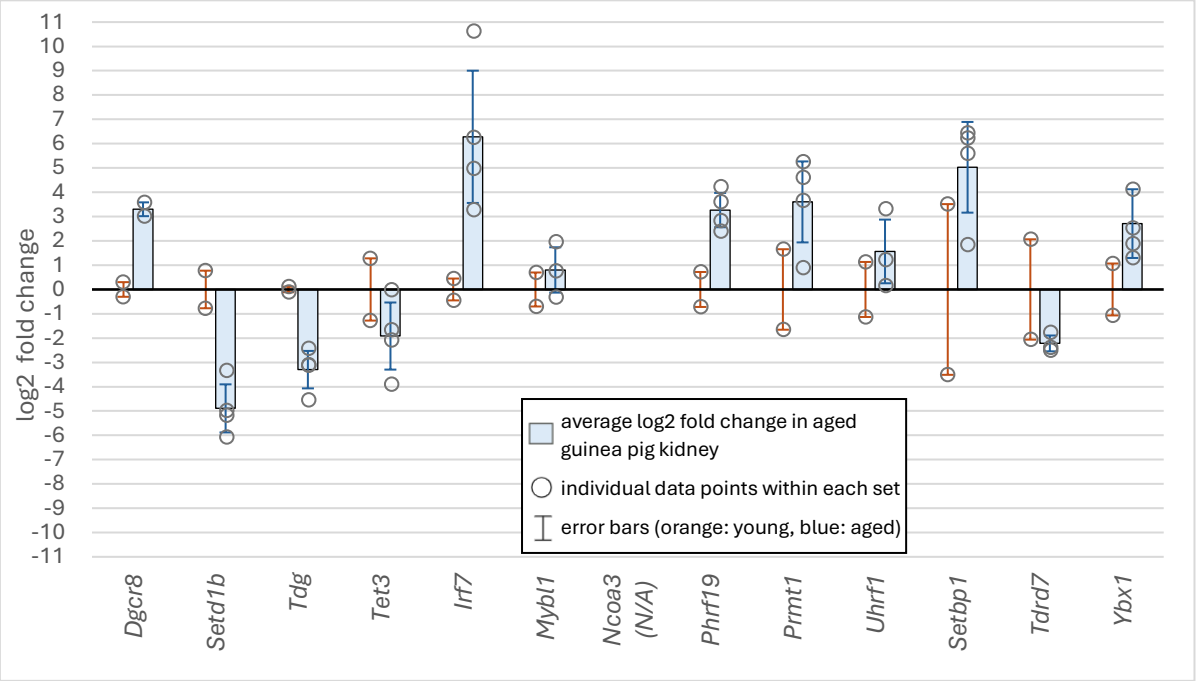

Figure 3 - Gene expression variability in guinea pig kidney. Blue error bars represent the standard deviation of the log2 fold change in aged to young. Orange error bars show the standard deviation within young individuals. N/A is not assessed.

The p-values used to distinguish between aged and young gene expression levels are presented in *Table 6.* None of the tested genes yielded p-values below the 0.05 significance threshold, indicating no statistically significant differences in gene expression levels between the aged and young groups. However, the lack of significant p-values may also be due to the smaller sample size, which can reduce the statistical power to detect differences.

Table 6 - Quantification cycle differences in guinea pig kidney and the p-values for statistical significance

KIDNEY	**ΔCq** (young)		**ΔCq** (aged)				
	YGP-1	**YGP-2**	**AGP-1**	**AGP-2**	**AGP-3**	**AGP-4**	**p-value**
Dgcr8	9.38	9.98	N/A	3.58	N/A	3.02	0.13
Setd1b	-6.32	-4.78	-2.22	-0.37	0.52	-0.57	0.13
Tdg	-5.19	-4.97	-0.54	-1.96	-1.98	-2.65	0.13
Tet3	3.37	0.81	4.17	3.75	5.99	2.11	0.13
Irf7	3.16	4.05	-1.37	-7.02	0.33	-2.65	0.13
Mybl1	7.96	6.56	7.58	N/A	6.49	5.29	0.13
Ncoa3	N/A	N/A	6.62	N/A	5.92	9.17	N/A
Phrf19	10.35	8.91	5.40	6.81	7.24	6.03	0.13
Prmt1	8.62	5.31	2.36	1.71	3.30	6.07	0.27
Uhrf1	5.10	2.84	2.74	N/A	3.81	0.66	0.40
Setbp1	-1.11	5.91	-3.83	0.56	-4.04	-3.20	0.27
Tdrd7	1.79	-2.33	2.11	N/A	2.24	1.49	0.40
Ybx1	-4.24	-2.11	-5.70	-4.47	-5.06	-7.30	0.20

Within the guinea pig kidney samples, although none of the results delivered statistically significant results, the overall trend in gene expression aligned with the expected bioinformatic predictions, with the exception of two genes. More specifically, the gene *Dgcr8* was found to be upregulated instead of downregulated, and the gene *Tdrd7* exhibited downregulation instead of upregulation. However, it is important to acknowledge that these trends may not be definitive due to the smaller sample size of young guinea pigs and the absence of statistical significance. Moreover, the results do not include *Ncoa3,* as this gene has not been successfully quantified.

4.2.3 Guinea pig liver

The log2 fold changes in the liver tissues of aged guinea pigs are depicted in *Figure 4*. Three genes, *Setd1b, Irf7* and *Setbp1,* are downregulated in aged guinea pig liver tissues, with the most profound gene expression decrease found in *Setbp1* with an average log2 fold change of -7.18. The most consistent downregulation is in *Setd1b,* while *Irf7* shows the most considerable variability by having the largest standard deviation among the three. Conversely, the gene *Prmt1* behaves differently as it has a consistent gene expression level across both age groups.

The other genes are upregulated, with average log2 fold changes ranging between 1.30 to 5.44. *Dgcr8* has the least significant upregulation with consistent results, and *Mybl1* has the most profound increase; however, this upregulation varies significantly. The genes *Tdrd7*, followed by *Uhrf1,* have the largest variability in log2 fold changes among all the tested genes in guinea pig liver samples. The quantification of gene expression levels of *Ncoa3* was successful in guinea pig livers, with only one of the aged samples without success.

In young guinea pig liver, the standard deviations of gene expression levels are the most consistent in the genes *Dgcr8, Tdg, Irf7, Ncoa3* and Setbp1, with *Ncoa3* having the lowest standard deviation with a value of 0.08. The highest standard deviations are found in the genes *Setd1b* and *Ybx1,* with values of 2.52 and 1.98, respectively.

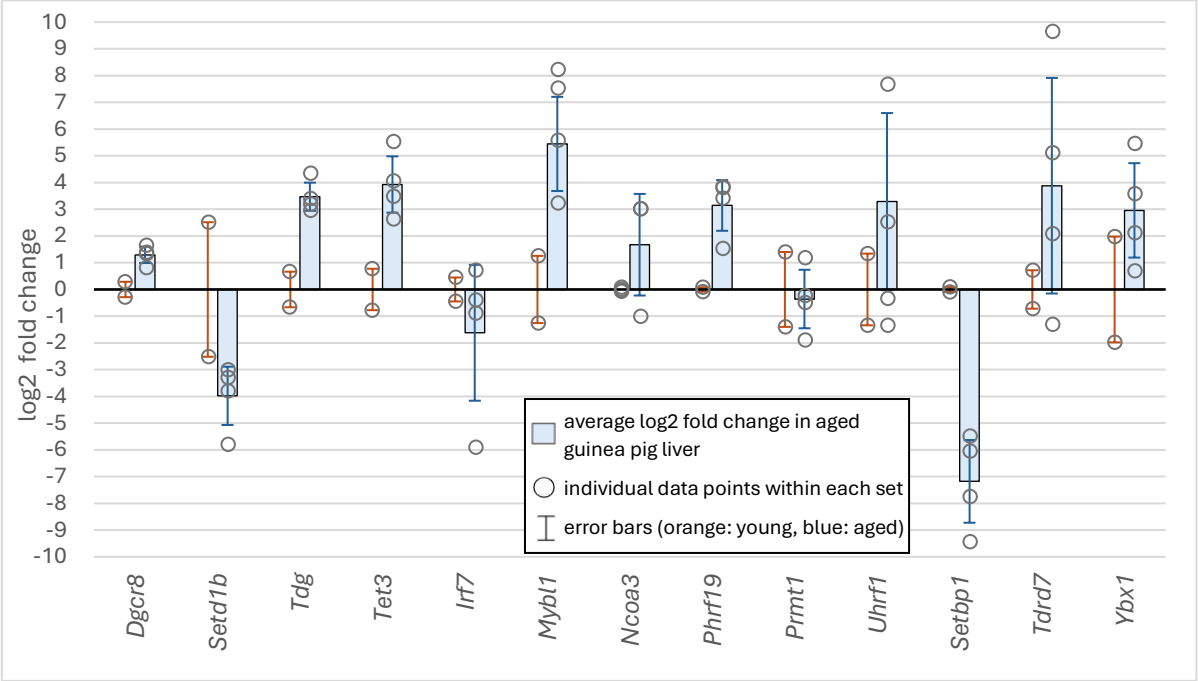

Figure 4 - Gene expression variability in guinea pig liver. Blue error bars represent the standard deviation of the log2 fold change in aged to young. Orange error bars show the standard deviation within young individuals.

Table 7 presents the p-values to compare gene expression levels between aged and young guinea pigs in the liver samples and the individual quantification cycle differences of each sample. None of the tested genes produced p-values below the 0.05 significance threshold, suggesting no statistically significant differences in gene expression between the two groups.

Table 7 - Quantification cycle differences in guinea pig liver and the p-values for statistical significance

LIVER	**ΔCq** (young)		**ΔCq** (aged)				
	YGP-1	**YGP-2**	**AGP-1**	**AGP-2**	**AGP-3**	**AGP-4**	**p-value**
Dgcr8	7.36	7.93	5.99	6.26	6.84	6.31	0.13
Setd1b	-6.34	-11.38	-5.85	-5.56	-3.06	-5.06	0.13
Tdg	4.13	2.80	0.07	0.27	0.51	-0.88	0.13
Tet3	7.86	6.31	3.60	1.56	4.45	3.03	0.13
Irf7	-8.49	-7.60	-2.14	-7.65	-7.15	-8.76	0.80
Mybl1	9.01	6.50	2.18	-0.46	4.53	0.23	0.13
Ncoa3	9.27	9.11	6.17	6.17	N/A	10.20	0.77
Phrf19	1.35	1.51	-0.10	-1.98	-2.37	-2.41	0.13
Prmt1	-5.88	-3.08	-2.59	-5.67	-3.99	-4.25	0.80
Uhrf1	-1.08	1.61	0.60	1.61	-2.26	-7.40	0.64
Setbp1	7.74	6.05	-7.74	-6.05	-9.44	-5.48	0.13
Tdrd7	-9.65	-5.11	9.65	5.11	2.08	-1.31	0.13
Ybx1	-6.92	-2.96	-8.52	-10.39	-5.63	-7.06	0.27

Interestingly, the guinea pig liver samples exhibited the highest divergence in gene expression patterns from the bioinformatic predictions, in contrast to the guinea pig kidney or mouse samples, where the gene expression trend largely matched the expectations. *Dgcr8, Tdg* and *Tet3* showed unexpected upregulation, whereas *Irf7, Prmt1* and *Setbp1* were downregulated instead of the anticipated upregulation. The genes not directly mentioned do behave as the predicted patterns. However, it is important to highlight that these results represent observed trends rather than definitive, statistically validated changes.

When comparing the expression level trends between the two organs, six genes behave similarly, and six behave differently. The differences include the upregulation of *Tdg* and *Tet3* in the aged liver samples and their downregulation in the aged kidney samples. Additionally, *Setd1b, Irf7* and *Setbp1* show a decreased expression in the aged liver samples and decreased expression in the aged kidney samples. *Prmt1* shows a consistent expression level across both age groups, with only a slight downregulation in the liver of aged guinea pigs but an upregulation in the kidneys. For *Ncoa3,* it was not possible to do a comparison between the two organs.

5. Discussion

The primary goal of this research was to validate previous bioinformatics results (Müller, 2022) concerning the relationship between epigenetic marks and mammalian lifespans. This was achieved by comparing gene expression levels of epigenetic factors in young and old-aged groups across different species and tissues. Our findings confirmed several gene expression trends previously observed and highlighted some discrepancies with earlier bioinformatics predictions from our laboratory. Our results support, to some extent, the hypothesis that gene expression levels change with age. The inconsistencies observed in our data, revealing variable gene expression levels, might stem from the complexity of epigenetic regulation.

The bioinformatics study hypothesised the downregulation of the genes *Dgcr8, Tdg, Tet3* and *Setd1b* in aged short-lived mammals. The observed trends of gene expression levels, derived from the experimental quantification of this study, largely confirm the expected downregulation of *Tdg, Tet3* and *Setd1b*. More precisely, the downregulation of these three genes was observed in the kidney tissues, with the decrease of *Tet3* being statistically significant and *Tdg* downregulation lying slightly above the statistical significance threshold. In the liver tissues of aged mice, only *Tet3* showed decreased expression from all the examined genes. The log2 fold changes between the aged and young guinea pig kidneys, corresponding to these three genes - *Tdg, Tet3* and *Setd1b* – also support their downregulation, with *Setd1b* showing the most compelling reduction within these three genes that primarily aligned with the expected downregulation trends. Furthermore, *Setd1b* was also found to have decreased levels in the aged guinea pig livers. Even though *Setd1b* was upregulated in aged mouse liver samples, this upregulation is quite inconsistent, indicated strongly by the outcomes of the statistical test. Therefore, the observed increase in *Setd1b* expression in aged mouse liver may be due to random variation. Interestingly, *Dgcr8* was consistently upregulated in all the samples, even though it was also anticipated to be downregulated. Although its upregulation was not statistically significant, it suggests a general pattern worth nothing. Moreover, this upregulation seemed relatively weak in aged guinea pig liver and aged mouse kidney, which might indicate that its expression does not change during ageing.

Based on the bioinformatics studies, the genes - *Irf7, Mybl1, Ncoa3, Phf19, Prmt1, Rnasel, Uhrf1, Setbp1, Tdrd7* and *Ybx1* - were anticipated to be upregulated in the samples belonging to aged individuals. Most results aligned with the expected outcomes, showing a general trend of increased gene expression in aged individuals. This upregulation was statistically

significant in the case of *Irf7* in both liver and kidney tissues of aged mouse samples, *Mybl1, Phrf19, Setbp1* and *Tdrd7* in aged mouse liver. In mouse kidney samples, the increased expression of *Rnasel* was statistically significant, and the upregulation of *Mybl1* was only slightly above the significant threshold level. Within all the samples, the upregulation of *Rnasel* was the most profound increase. However, it is also important to note that the expression levels of *Irf7, Setbp1* and *Tdrd7* reduced in one of the organs of guinea pigs. This unexpected downregulation was most profound in the case of *Setbp1* in aged guinea pig liver. In the same tissues, the expression levels of *Irf7* also fell. *Tdrd7* levels were found to be reduced in aged guinea pig kidneys.

Additionally, the observed upregulation trend of *Prmt1* and *Setbp1* was relatively minimal in aged mouse kidneys, suggesting that these genes may not be upregulated here. Instead, they remain consistently expressed across the two age groups. Furthermore, the negligible decrease of *Prmt1,* observed in aged mouse liver tissues, and the corresponding statistical analysis showing a large variability of log2 fold change differences indicates that this gene remains constantly expressed in mice. Moreover, *Prtm1* again showed a consistent expression pattern in aged guinea pig liver; however, this time, it was due to an insignificant reduction in its level.

The genes of this study encode epigenetic factors that either contribute to the heterochromatin or euchromatin maintenance or facilitate diverse DNA repair processes, all of which are strongly influenced by the organism's age. Overall, the natural biological decline and the ageing process are strongly associated with changes in chromatin driven by epigenetic modifications. More specifically, ageing is associated with the overall loss of heterochromatin, which essentially transforms into its open and active euchromatin form (Zhang et al.,2020). This process is facilitated by changes in histone modification patterns and a general loss of histone proteins (Pal & Tyler, 2016). Moreover, a noticeable trend of localised DNA hypomethylation within the GpC islands is also common (Fraga et al., 2007). All these modifications contribute to altered gene regulation and declining genetic instability of the cells (Mutirangura, 2019). Remodelled expression of epigenetic factors can contribute to this dysregulation so that tightly packed chromatin becomes more open and vice versa. Although the changes are random to some extent and vary from cell to cell, they predominantly impact cell health negatively (Saul & Kosinsky, 2021).

The findings of this study support this dysregulation. For instance, the genes *Tet3* (Ito et al., 2011) and *Tdg* (Cortellino et al., 2011) facilitate the DNA demethylation process, whereas *Setd1b* encodes a histone methyltransferase protein responsible for trimethylating the H3K4

position (Nacarelli et al., 2022). All three genes, therefore, support the open chromatin conformation. The observed trend in reduction in the expression of these three genes might impair the proper maintenance of euchromatin. Moreover, *Tdg* encodes an enzyme crucial in the base excision repair cell (Dalton & Bellacosa, 2012). The catalytic activity of TET3 has also been found to be essential in repairing DNA upon cell damage (Jiang et al., 2017). Overall, the reduced expression of these genes leads to a deterioration in proper DNA repair and even preserving cell homeostasis. This is in correlation with genomic instability that is to be anticipated with ageing (López-Gil et al., 2023).

In contrast, DGCR8 stabilises the heterochromatin conformation through its interaction with various heterochromatin-associated proteins using its unique motifs that are located at its N-terminus (Deng et al., 2019). Its consistent upregulation in aged samples might suggest a possible compensatory response to counteract the declining genomic stability caused by the general trend of heterochromatin loss observed during ageing (Zhang et al., 2020). Overexpressing *Dgcr8* might be an adaptive response as it has been shown that heterochromatin stabilisation can mitigate cellular senescence (Deng et al., 2019).

Several genes had been statistically significantly upregulated in at least one sample batch, which may contribute to unusual gene expression patterns or mitigate cellular stress with ageing. Generally, the upregulation of genes that counteract increased inflammatory signalling and oxidative stress is observed in aged tissues (Zuo et al., 2019). This suggests that the activation of these genes might increase as a response to external pathogens, whose presence poses a greater risk to the organisms as they age. For example, the gene *Irf7* - found to be statistically significantly upregulated in both organs of aged mice - encodes a transcription factor, which binds the DNA using its helix-turn-helix turn motif to initiate type 1 interferon immune response. Epigenetic post-translational modifications of IRF7, such as acetylation by acetyltransferases, can regulate its activation and DNA-binding capability (Ma et al., 2023). Activated RNASEL degrades viral RNA molecules by acting as a regulator of type 1 interferon immune response (Silverman, 2007). Moreover, RNASEL has been linked to the cleavage of mRNA molecules, thereby indirectly controlling the translation of the proteins they encode (Brennan-Laun et al., 2014). TDRD7 assists in the suppression of viral proliferation (Chakravarty et al., 2023). Furthermore, it contains a Tudor domain (Chakravarty et al., 2023), which can recognise methylated lysine or arginine residues of histones, thereby acting as a methylation marker reader (Scheid et al., 2021). In addition, both *Uhrf1* and *Phf19* encode proteins that contain these domains. Tudor-containing proteins can recognise methylation

marks and recruit further protein complexes to alter the chromatin structure (Lu & Wang, 2013).

The upregulation of *Setbp1* in aged individuals could induce aberrant gene expression patterns, as this gene is known to encode transcriptional co-activator, which assists the binding of AT-rich promoter regions. This facilitates the recruitment of various epigenetic complexes associated with increased gene expression (Piazza et al., 2018). *Mybl1* encodes a transcription factor that has also been associated with increasing gene expression levels (Xie et al., 2020), potentially contributing to genetic instability in aged cells when overexpressed. The encoded protein belongs to the MYB transcription factors, which can bind DNA with specific binding motifs located at their conserved N-terminus (Anand et al., 2024).

The profound variabilities observed in gene expression patterns upon quantifying the same gene can be biological, attributed to the complex interplay of genetic regulatory mechanisms, or technical, caused by experimental errors such as primer inefficiency or pipetting inaccuracies that can affect cDNA yield and the PCR amplification product. To avoid the potential problems with the employed primers, one should test primer efficiency on serial dilutions of cDNA. For instance, several amplification cycles in the guinea pig samples exceeded the qPCR cycle threshold, indicating that the gene was undetected. Consequently, the gene *Ncoa3* was not quantifiable in the guinea pig kidney samples, and a few other genes also produced limited data due to the similar non-detection across different runs. This persistent problem, especially in guinea pig samples, might stem from low-quality RNA due to possible contaminations by PCR inhibitors. These inhibitors are known to influence the reliability of the quantification results negatively (Cai et al., 2018). Even though the absorption rates of cDNA indicate the absence of contaminants, some inhibitors might have been co-extracted with RNA and still present at low levels during the quantitative PCR runs. Despite efforts to resolve these issues, including using new reagents and the re-synthesis and re-testing of a fresh batch of cDNA, the results did not improve. Further examination with gel electrophoresis carried out with a few of the qPCR amplification products confirmed that only one product of the expected size had been synthesised, which rules out non-specific binding or primer-primer dimer formation. However, despite this, the guinea pig primer design could still play a significant role in these outcomes as they were chosen to align as perfectly as possible with the mouse gene primers. Additional steps would be needed to improve the experimental outcomes, mainly to redesign the primers and redo the RNA extraction from new samples. These challenges also led to the absence of statistically significant changes in the gene expression levels obtained in aged guinea pig tissues. The already smaller sample of

young guinea pigs made it less likely to achieve statistically significant results. Additionally., the possibly poor quality of the RNA further decreased the chances of identifying significant differences.

To establish a unique correlation between the expression levels of these epigenetic factors and the animal's lifespan, further research is necessary. This could expand on the findings of this study by incorporating additional species, organs and larger sample sizes to improve the generalisability of the results. The follow-up study of this project will include analysing the gene expression levels in African mole-rat (*Bathyergidae*) organs, which is an essential step as during this current study, we were unable to conduct the planned quantitative analysis of long-lived giant mole-rats (*Fukomys mechowii*). These animals, and other related species, such as the naked mole-rats (*Heterocephalus glaber*), present unique opportunities for studying epigenetic expression patterns correlated to enhanced longevity and resistance to age-related diseases (Sahm et al., 2018). Their longevity is also linked to lower metabolic rates and a stable environment in their underground lifestyle, which reduces stress and oxidative damage compared to terrestrial animals (Johansen' et al., 1976).

As these epigenetic regulatory mechanisms that influence life span and healthy ageing are remarkably complex, further studies are crucial to explore and understand how these precise regulatory patterns can promote epigenomic and genomic stability and cellular homeostasis. Moreover, the disruption of the epigenomic landscape associated with ageing causes irregular gene expression patterns, which contribute to ageing-associated phenotypes (Li & Tollefsbol, 2016). While current research has succeeded in gathering partial information on the epigenetic landscape, there remains a need for a comprehensive understanding of how epigenetic regulatory mechanisms span across various stages of life (Henikoff, 2023). Such extensive information could offer insights into how epigenetic marks evolve and how these changes correlate with physiological and pathological ageing processes (Horvath & Raj, 2018). Furthermore, there is a limited understanding of the functional consequences of the ageing-related epigenetic DNA methylation processes (Jones et al., 2015). A more profound comprehension of the chronological and biological aspects of an organism's epigenetic landscape could help identify potential biomarkers for ageing and improve treatment strategies (Bell et al., 2019).

Another promising area of research is the connection between epigenetics and environmental factors concerning ageing. Lifestyle factors such as diet, exercise and exposure to toxins have been shown to influence epigenetic marks. These changes can have lasting effects on the

overall health and the healthy ageing process (Mathers et al., 2010). Future studies should aim to study how these different environmental factors interact with the epigenome. Such research could assist in developing personalised lifestyles that promote healthy ageing by optimising the epigenetic landscape (Feinberg & Fallin, 2015).

Ultimately, future research might deepen our understanding of how these epigenetic marks of longevity and ageing can contribute to preventing the age-linked decline of an organism. By identifying the involved pathways, these could be adjusted to promote healthy ageing and potentially increase lifespan.

6. References

Anand, S., Vikramdeo, K. S., Sudan, S. K., Sharma, A., Acharya, S., Khan, M. A., Singh, S., & Singh, A. P. (2024). From modulation of cellular plasticity to potentiation of therapeutic resistance: new and emerging roles of MYB transcription factors in human malignancies. *Cancer metastasis reviews*, *43*(1), 409–421. https://doi.org/10.1007/s10555-023-10153-8

Anand, D., Al Saai, S., Shrestha, S. K., Barnum, C. E., Chuma, S., & Lachke, S. A. (2021). Genome-Wide Analysis of Differentially Expressed miRNAs and Their Associated Regulatory Networks in Lenses Deficient for the Congenital Cataract-Linked Tudor Domain Containing Protein TDRD7. *Frontiers in Cell and Developmental Biology*, *9*, 615761. https://doi.org/10.3389/fcell.2021.615761

Andersen, J. B., Li, X. L., Judge, C. S., Zhou, A., Jha, B. K., Shelby, S., Zhou, L., Silverman, R. H., & Hassel, B. A. (2007). Role of 2-5A-dependent RNase-L in senescence and longevity. *Oncogene*, *26*(21), 3081-3088. https://doi.org/10.1038/sj.onc.1210111

Ballaré, C., Lange, M., Lapinaite, A., Martin, G. M., Morey, L., Pascual, G., Liefke, R., Simon, B., Shi, Y., Gozani, O., Carlomagno, T., Benitah, S. A., & Di Croce, L. (2012). Phf19 links methylated Lys36 of histone H3 to regulation of Polycomb activity. *Nature Structural & Molecular Biology*, *19*(12), 1257-1265. https://doi.org/10.1038/nsmb.2434

Barker, S. J., & Tsai, L. H. (2017). MethyLock: DNA Demethylation Is the Epigenetic Key to Axon Regeneration. *Neuron*, *94*(2), 221–223. https://doi.org/10.1016/j.neuron.2017.04.006

Beacon, T. H., Delcuve, G. P., López, C., Nardocci, G., Kovalchuk, I., van Wijnen, A. J., & Davie, J. R. (2021). The dynamic broad epigenetic (H3K4me3, H3K27ac) domain as a mark of essential genes. *Clinical epigenetics*, *13*(1), 138. https://doi.org/10.1186/s13148-021-01126-1

Bell, C. G., Lowe, R., Adams, P. D., Baccarelli, A. A., Beck, S., Bell, J. T., Christensen, B. C., Gladyshev, V. N., Heijmans, B. T., Horvath, S., Ideker, T., Issa, J. J., Kelsey, K. T., Marioni, R. E., Reik, W., Relton, C. L., Schalkwyk, L. C., Teschendorff, A. E., Wagner, W., Zhang, K., … Rakyan, V. K. (2019). DNA methylation aging clocks: challenges and recommendations. *Genome biology*, *20*(1), 249. https://doi.org/10.1186/s13059-019-1824-y

Benayoun, B. A., Pollina, E. A., Singh, P. P., Mahmoudi, S., Harel, I., Casey, K. M., Dulken, B. W., Kundaje, A., & Brunet, A. (2019). Remodeling of epigenome and transcriptome landscapes with aging in mice reveals widespread induction of inflammatory responses. *Genome research*, *29*(4), 697–709. https://doi.org/10.1101/gr.240093.118

Bińkowski, J., Taryma-Leśniak, O., Łuczkowska, K., Niedzwiedź, A., Lechowicz, K., Strapagiel, D., Jarczak, J., Davalos, V., Pujol, A., Esteller, M., Kotfis, K., Machaliński, B., Parczewski, M., & Wojdacz, T. K. (2022). Epigenetic activation of antiviral sensors and effectors of interferon response pathways during SARS-CoV-2 infection. *Biomedicine & Pharmacotherapy*, *153*, 113396. https://doi.org/10.1016/j.biopha.2022.113396

Bogliotti, Y. S., & Ross, P. J. (2012). Mechanisms of histone H3 lysine 27 trimethylation remodeling during early mammalian development. *Epigenetics*, *7*(9), 976-981. https://doi.org/10.4161/epi.21615

Bönisch, C., & Hake, S. B. (2012). Histone H2A variants in nucleosomes and chromatin: More or less stable? *Nucleic Acids Research*, *40*(21), 10719-10741. https://doi.org/10.1093/nar/gks865

Brennan-Laun, S. E., Ezelle, H. J., Li, L., & Hassel, B. A. (2014). RNase-L Control of Cellular mRNAs: Roles in Biologic Functions and Mechanisms of Substrate Targeting. *Journal of Interferon & Cytokine Research*, *34*(4), 275-288. https://doi.org/10.1089/jir.2013.0147

Broberg, K., Engström, K., & Ameer, S. (2014). Gene-Environment Interactions for Metals. In G. Nordberg, B. Fowler, & M. Nordberg (Eds.), *Handbook on the Toxicology of Metals* (4th ed., Vol. 1, pp. 239-264). Academic Press. https://doi.org/10.1016/B978-0-444-59453-2.00012-3

Brunner, A. M., Nanni, P., & Mansuy, I. M. (2014). Epigenetic marking of sperm by post-translational modification of histones and protamines. *Epigenetics & chromatin*, *7*(1), 2. https://doi.org/10.1186/1756-8935-7-2

Cai, D., Behrmann, O., Hufert, F., Dame, G., & Urban, G. (2018). Direct DNA and RNA detection from large volumes of whole human blood. *Scientific Reports*, *8*(1), 1-9. https://doi.org/10.1038/s41598-018-21224-0

Chakravarty, S., Subramanian, G., Popli, S., Veleeparambil, M., Fan, S., Chakravarti, R., & Chattopadhyay, S. (2023). Interferon-stimulated gene TDRD7 interacts with AMPK and

inhibits its activation to suppress viral replication and pathogenesis. *mBio*, *14*(5), e0061123. https://doi.org/10.1128/mbio.00611-23

Cortázar, D., Kunz, C., Selfridge, J., Lettieri, T., Saito, Y., MacDougall, E., Wirz, A., Schuermann, D., Jacobs, A. L., Siegrist, F., Steinacher, R., Jiricny, J., Bird, A., & Schär, P. (2011). Embryonic lethal phenotype reveals a function of TDG in maintaining epigenetic stability. *Nature*, *470*(7334), 419-423. https://doi.org/10.1038/nature09672

Cortellino, S., Xu, J., Sannai, M., Moore, R., Caretti, E., Cigliano, A., Le Coz, M., Devarajan, K., Wessels, A., Soprano, D., Abramowitz, L. K., Bartolomei, M. S., Rambow, F., Bassi, M. R., Bruno, T., Fanciulli, M., Renner, C., Klein-Szanto, A. J., Matsumoto, Y., Kobi, D., … Bellacosa, A. (2011). Thymine DNA glycosylase is essential for active DNA demethylation by linked deamination-base excision repair. *Cell*, *146*(1), 67–79. https://doi.org/10.1016/j.cell.2011.06.020

Dalton, S. R., & Bellacosa, A. (2012). DNA demethylation by TDG. *Epigenomics*, *4*(4), 459–467. https://doi.org/10.2217/epi.12.36

Deaton, A. M., & Bird, A. (2011). CpG islands and the regulation of transcription. *Genes & development*, *25*(10), 1010–1022. https://doi.org/10.1101/gad.2037511

Deng, L., Ren, R., Liu, Z., Song, M., Li, J., Wu, Z., Ren, X., Fu, L., Li, W., Zhang, W., Guillen, P., Izpisua Belmonte, J. C., Chan, P., Qu, J., & Liu, G. (2019). Stabilizing heterochromatin by DGCR8 alleviates senescence and osteoarthritis. *Nature Communications*, *10*(1), 1-16. https://doi.org/10.1038/s41467-019-10831-8

Dinh, N. T., Nguyen, T. M., Park, M. K., & Lee, C. H. (2023). Y-Box Binding Protein 1: Unraveling the Multifaceted Role in Cancer Development and Therapeutic Potential. *International Journal of Molecular Sciences*, *25*(2), 717. https://doi.org/10.3390/ijms25020717

Domcke, S., Bardet, A. F., Adrian Ginno, P., Hartl, D., Burger, L., & Schübeler, D. (2015). Competition between DNA methylation and transcription factors determines binding of NRF1. *Nature*, *528*(7583), 575-579. https://doi.org/10.1038/nature16462

D'Orazio, F. M., Balwierz, P. J., González, A. J., Guo, Y., Hernández-Rodríguez, B., Wheatley, L., Jasiulewicz, A., Hadzhiev, Y., Vaquerizas, J. M., Cairns, B., Lenhard, B., & Müller, F. (2021). Germ cell differentiation requires Tdrd7-dependent chromatin and transcriptome

reprogramming marked by germ plasm relocalization. *Developmental cell*, *56*(5), 641–656. https://doi.org/10.1016/j.devcel.2021.02.007

Draker, R., & Cheung, P. (2009). Transcriptional and epigenetic functions of histone variant H2A.Z. *Biochemistry and cell biology = Biochimie et biologie cellulaire, 87*(1), 19–25. https://doi.org/10.1139/O08-117

Feinberg, A. P., & Fallin, M. D. (2015). Epigenetics at the Crossroads of Genes and the Environment. *JAMA*, *314*(11), 1129. https://doi.org/10.1001/jama.2015.10414

Field, A. E., Robertson, N. A., Wang, T., Havas, A., Ideker, T., & Adams, P. D. (2018). DNA Methylation Clocks in Aging: Categories, Causes, and Consequences. *Molecular cell, 71*(6), 882–895. https://doi.org/10.1016/j.molcel.2018.08.008

Fraga, M. F., Agrelo, R., & Esteller, M. (2007). Cross-talk between aging and cancer: the epigenetic language. *Annals of the New York Academy of Sciences, 1100,* 60–74. https://doi.org/10.1196/annals.1395.005

Gázquez-Gutiérrez, A., Witteveldt, J., Heras, S. R., & Macias, S. (2021). Sensing of transposable elements by the antiviral innate immune system. *RNA*, *27*(7), 735-752. https://doi.org/10.1261/rna.078721.121

Gentilini, D., Mari, D., Castaldi, D., Remondini, D., Ogliari, G., Ostan, R., Bucci, L., Sirchia, S. M., Tabano, S., Cavagnini, F., Monti, D., Franceschi, C., Di Blasio, A. M., & Vitale, G. (2013). Role of epigenetics in human aging and longevity: Genome-wide DNA methylation profile in centenarians and centenarians' offspring. *Age, 35*(5), 1961–1973. https://doi.org/10.1007/s11357-012-9463-1

Ghamlouch, H., Boyle, E. M., Blaney, P., Wang, Y., Choi, J., Williams, L., Bauer, M., Auclair, D., Bruno, B., Walker, B. A., Davies, F. E., & Morgan, G. J. (2021). Insights into high-risk multiple myeloma from an analysis of the role of PHF19 in cancer. *Journal of experimental & clinical cancer research : CR*, *40*(1), 380. https://doi.org/10.1186/s13046-021-02185-1

Giaimo, B. D., Ferrante, F., Herchenröther, A., Hake, S. B., & Borggrefe, T. (2019). The histone variant H2A.Z in gene regulation. *Epigenetics & chromatin*, *12*(1), 37. https://doi.org/10.1186/s13072-019-0274-9

Guo, H., Zhang, B., Nairn, A. V., Nagy, T., Moremen, K. W., Buckhaults, P., & Pierce, M. (2017). *O*-Linked *N*-Acetylglucosamine (*O*-GlcNAc) Expression Levels Epigenetically

Regulate Colon Cancer Tumorigenesis by Affecting the Cancer Stem Cell Compartment via Modulating Expression of Transcriptional Factor *MYBL1*. *The Journal of biological chemistry*, *292*(10), 4123–4137. https://doi.org/10.1074/jbc.M116.763201

Guo, S. W. (2012). The Epigenetics of Endometriosis. *Epigenetics in Human Disease* (pp. 443–469). Academic Press. https://doi.org/10.1016/B978-0-12-388415-2.00022-6

Hassan, H. M., Isovic, M., Kolendowski, B., Bauer-Maison, N., Onabote, O., Cecchini, M., Haig, A., Maleki Vareki, S., Underhill, T. M., & Torchia, J. (2020). Loss of Thymine DNA Glycosylase Causes Dysregulation of Bile Acid Homeostasis and Hepatocellular Carcinoma. *Cell reports, 31*(1), 107475. https://doi.org/10.1016/j.celrep.2020.03.039

Henikoff, S. (2023). The epigenetic landscape: An evolving concept. *Frontiers in Epigenetics and Epigenomics*, *1*, 1176449. https://doi.org/10.3389/freae.2023.1176449

Hillman SC, Dale J. (2018). Epigenetics. *InnovAiT*, *11*(12), 689-692. https://doi:10.1177/1755738018796032

Horvath S. (2013). DNA methylation age of human tissues and cell types. *Genome biology, 14*(10), 3156. https://doi.org/10.1186/gb-2013-14-10-r115

Horvath, S., & Raj, K. (2018). DNA methylation-based biomarkers and the epigenetic clock theory of ageing. Nature reviews. *Genetics*, *19*(6), 371–384. https://doi.org/10.1038/s41576-018-0004-3

Huisinga, K. L., Brower-Toland, B., & Elgin, S. C. (2006). The contradictory definitions of heterochromatin: transcription and silencing. *Chromosoma, 115*(2), 110–122. https://doi.org/10.1007/s00412-006-0052-x

Ito, S., Shen, L., Dai, Q., Wu, S. C., Collins, L. B., Swenberg, J. A., He, C., & Zhang, Y. (2011). Tet proteins can convert 5-methylcytosine to 5-formylcytosine and 5-carboxylcytosine. *Science (New York, N.Y.)*, *333*(6047), 1300–1303. https://doi.org/10.1126/science.1210597

Johansen, K., Lykkeboe, G., Weber, R. E., & Maloiy, G. M. (1976). Blood respiratory properties in the naked mole rat Heterocephalus glaber, a mammal of low body temperature. *Respiration physiology*, *28*(3), 303–314. https://doi.org/10.1016/0034-5687(76)90025-6

Jones, M. J., Goodman, S. J., & Kobor, M. S. (2015). DNA methylation and healthy human aging. *Aging cell, 14*(6), 924–932. https://doi.org/10.1111/acel.12349

Jiang, D., Wei, S., Chen, F., Zhang, Y., & Li, J. (2017). TET3-mediated DNA oxidation promotes ATR-dependent DNA damage response. *EMBO Reports*, *18*(5), 781-796. https://doi.org/10.15252/embr.201643179

Jin, B., Li, Y., & Robertson, K. D. (2011). DNA methylation: superior or subordinate in the epigenetic hierarchy?. *Genes & cancer, 2*(6), 607–617. https://doi.org/10.1177/1947601910393957

Kiefer J. C. (2007). Epigenetics in development. *Developmental dynamics : an official publication of the American Association of Anatomists, 236*(4), 1144–1156. https://doi.org/10.1002/dvdy.21094

Kim, B. M., Hong, Y., Lee, S., Liu, P., Lim, J. H., Lee, Y. H., Lee, T. H., Chang, K. T., & Hong, Y. (2015). Therapeutic Implications for Overcoming Radiation Resistance in Cancer Therapy. *International Journal of Molecular Sciences*, *16*(11), 26880-26913. https://doi.org/10.3390/ijms161125991

Kocić, G., Hadzi-Djokić, J., Veljković, A., Roumeliotis, S., Janković-Veličković, L., & Šmelcerović, A. (2022). Template-Independent Poly(A)-Tail Decay and RNASEL as Potential Cellular Biomarkers for Prostate Cancer Development. *Cancers, 14*(9), 2239. https://doi.org/10.3390/cancers14092239

Kostyrko, K., Román, M., Lee, A. G., Simpson, D. R., Dinh, P. T., Leung, S. G., Marini, K. D., Kelly, M. R., Broyde, J., Califano, A., Jackson, P. K., & Sweet-Cordero, E. A. (2023). UHRF1 is a mediator of KRAS driven oncogenesis in lung adenocarcinoma. *Nature communications, 14*(1), 3966. https://doi.org/10.1038/s41467-023-39591-2

Krzyzewska, I. M., Maas, S. M., Henneman, P., Lip, K. V. D., Venema, A., Baranano, K., Chassevent, A., Aref-Eshghi, E., van Essen, A. J., Fukuda, T., Ikeda, H., Jacquemont, M., Kim, H. G., Labalme, A., Lewis, S. M. E., Lesca, G., Madrigal, I., Mahida, S., Matsumoto, N., Rabionet, R., … Mannens, M. M. A. M. (2019). A genome-wide DNA methylation signature for SETD1B-related syndrome. *Clinical epigenetics, 11*(1), 156. https://doi.org/10.1186/s13148-019-0749-3

Kuwano, M., Shibata, T., Watari, K., & Ono, M. (2019). Oncogenic Y-box binding protein-1 as an effective therapeutic target in drug-resistant cancer. *Cancer science, 110*(5), 1536–1543. https://doi.org/10.1111/cas.14006

Li, E., & Zhang, Y. (2014). DNA methylation in mammals. *Cold Spring Harbor perspectives in biology, 6*(5), 019133. https://doi.org/10.1101/cshperspect.a019133

Li, Y., & Tollefsbol, T. O. (2016). Age-related epigenetic drift and phenotypic plasticity loss: Implications in prevention of age-related human diseases. *Epigenomics*, 8(12), 1637-1651. https://doi.org/10.2217/epi-2016-007

Lieberman P. M. (2008). Chromatin organization and virus gene expression. *Journal of cellular physiology, 216*(2), 295–302. https://doi.org/10.1002/jcp.21421

Linder, K., Iragavarapu, C. & Liu, D. (2017). SETBP1 mutations as a biomarker for myelodysplasia/ myeloproliferative neoplasm overlap syndrome. *Biomark Research, 5*, 33. https://doi.org/10.1186/s40364-017-0113-8

Lim, J. P., Shyamasundar, S., Gunaratne, J., Scully, O. J., Matsumoto, K., & Bay, B. H. (2017). YBX1 gene silencing inhibits migratory and invasive potential via CORO1C in breast cancer in vitro. *BMC cancer, 17*(1), 201. https://doi.org/10.1186/s12885-017-3187-7

López-Gil, L., Pascual-Ahuir, A., & Proft, M. (2023). Genomic Instability and Epigenetic Changes during Aging. *International journal of molecular sciences*, *24*(18). https://doi.org/10.3390/ijms241814279

Lio, C. J., & Rao, A. (2019). TET Enzymes and 5hmC in Adaptive and Innate Immune Systems. *Frontiers in immunology, 10.* https://doi.org/10.3389/fimmu.2019.00210

Lu, R., & Wang, G. G. (2013). Tudor: A versatile family of histone methylation 'readers'. *Trends in Biochemical Sciences*, *38*(11). https://doi.org/10.1016/j.tibs.2013.08.002

Luger, K., Mäder, A. W., Richmond, R. K., Sargent, D. F., & Richmond, T. J. (1997). Crystal structure of the nucleosome core particle at 2.8 A resolution. *Nature, 389*(6648), 251–260. https://doi.org/10.1038/38444

Ma, W., Huang, G., Wang, Z., Wang, L., & Gao, Q. (2023). IRF7: role and regulation in immunity and autoimmunity. *Frontiers in immunology, 14.* https://doi.org/10.3389/fimmu.2023.1236923

Mariño-Ramírez, L., Kann, M. G., Shoemaker, B. A., & Landsman, D. (2005). Histone structure and nucleosome stability. *Expert review of proteomics, 2*(5), 719–729. https://doi.org/10.1586/14789450.2.5.719

Mathers, J. C., Strathdee, G., & Relton, C. L. (2010). Induction of epigenetic alterations by dietary and other environmental factors. *Advances in genetics*, *71*, 3–39. https://doi.org/10.1016/B978-0-12-380864-6.00001-8

Musiani, D., Giambruno, R., Massignani, E., Nicosia, L., Pasini, D., & Correspondence, T. B. (2020). PRMT1 Is Recruited via DNA-PK to Chromatin Where It Sustains the Senescence-Associated Secretory Phenotype in Response to Cisplatin. *CellReports, 30*, 1208-1222. https://doi.org/10.1016/j.celrep.2019.12.061

Müller, M. (2022). Multispecies analysis of the role of epigenetic factors in ageing. [Bachelor's thesis, University of South Bohemia]

Mutirangura, A. (2019). A Hypothesis to Explain How the DNA of Elderly People Is Prone to Damage: Genome-Wide Hypomethylation Drives Genomic Instability in the Elderly by Reducing Youth-Associated Gnome-Stabilizing DNA Gaps. IntechOpen. https://doi.org/10.5772/intechopen.83372

Nacarelli, T., Azar, A., Potnis, M., Johannes, G., Mell, J., Johnson, F. B., Brown-Borg, H., Noguchi, E., & Sell, C. (2022). The methyltransferase enzymes KMT2D, SETD1B, and ASH1L are key mediators of both metabolic and epigenetic changes during cellular senescence. *Molecular biology of the cell, 33*(5). https://doi.org/10.1091/mbc.E20-08-0523

Newkirk, S. J., & An, W. (2020). UHRF1: a jack of all trades, and a master epigenetic regulator during spermatogenesis. *Biology of reproduction, 102*(6), 1147–1152. https://doi.org/10.1093/biolre/ioaa026

Ninova, M., Fejes Tóth, K., & Aravin, A. A. (2019). The control of gene expression and cell identity by H3K9 trimethylation. *Development, 146*(19). https://doi.org/10.1242/dev.181180

Nodari, A., Scambi, I., Peroni, D., Calabria, E., Benati, D., Mannucci, S., Manfredi, M., Frontini, A., Visonà, S., Bozzato, A., Sbarbati, A., Schena, F., Marengo, E., Krampera, M., & Galiè, M. (2021). Interferon regulatory factor 7 impairs cellular metabolism in aging adipose-derived stromal cells. *Journal of cell science, 134*(11). https://doi.org/10.1242/jcs.256230

Onabote, O., Hassan, H. M., Isovic, M., & Torchia, J. (2022). The Role of Thymine DNA Glycosylase in Transcription, Active DNA Demethylation, and Cancer. *Cancers, 14*(3). https://doi.org/10.3390/cancers14030765

Pagiatakis, C., Musolino, E., Gornati, R., Bernardini, G., & Papait, R. (2021). Epigenetics of aging and disease: a brief overview. *Aging clinical and experimental research, 33*(4), 737–745. https://doi.org/10.1007/s40520-019-01430-0

Pal, S., & Tyler, J. K. (2016). Epigenetics and aging. *Science advances, 2*(7). https://doi.org/10.1126/sciadv.1600584

Papait, R., Corrado, N., Rusconi, F., Serio, S., & V G Latronico, M. (2015). It's Time for An Epigenomics Roadmap of Heart Failure. *Current genomics, 16*(4), 237–244. https://doi.org/10.2174/1389202916666150505183624

Piazza, R., Magistroni, V., Redaelli, S., Mauri, M., Massimino, L., Sessa, A., Peronaci, M., Lalowski, M., Soliymani, R., Mezzatesta, C., Pirola, A., Banfi, F., Rubio, A., Rea, D., Stagno, F., Usala, E., Martino, B., Campiotti, L., Merli, M., … Gambacorti-Passerini, C. (2018). SETBP1 induces transcription of a network of development genes by acting as an epigenetic hub. *Nature Communications, 9*(1), 1–13. https://doi.org/10.1038/s41467-018-04462-8

Redon, C., Pilch, D., Rogakou, E., Sedelnikova, O., Newrock, K., & Bonner, W. (2002). Histone H2A variants H2AX and H2AZ. *Current opinion in genetics & development, 12*(2), 162–169. https://doi.org/10.1016/s0959-437x(02)00282-4

Robertson K. D. (2005). DNA methylation and human disease. Nature reviews. *Genetics, 6*(8), 597–610. https://doi.org/10.1038/nrg1655

Rodríguez-Rodero, S., Fernández-Morera, J. L., Menéndez-Torre, E., Calvanese, V., Fernández, A. F., & Fraga, M. F. (2011). Aging genetics and aging. *Aging and disease, 2*(3), 186–195.

Sahm, A., Bens, M., Szafranski, K., Holtze, S., Groth, M., Görlach, M., Calkhoven, C., Müller, C., Schwab, M., Kraus, J., Kestler, H. A., Cellerino, A., Burda, H., Hildebrandt, T., Dammann, P., & Platzer, M. (2018). Long-lived rodents reveal signatures of positive selection in genes associated with lifespan. *PLoS genetics, 14*(3). https://doi.org/10.1371/journal.pgen.1007272

Salzberg, A. C., Harris-Becker, A., Popova, E. Y., Keasey, N., Loughran, T. P., Claxton, D. F., & Grigoryev, S. A. (2017). Genome-wide mapping of histone H3K9me2 in acute myeloid leukemia reveals large chromosomal domains associated with massive gene silencing and sites of genome instability. *PloS one, 12*(3). https://doi.org/10.1371/journal.pone.0173723

Sarkar, D., Sharma, R., Singh, P., Verma, V., Karkhur, S., Verma, S., Soni, D., & Sharma, B. (2023). Age-related cataract - Prevalence, epidemiological pattern and emerging risk factors in a cross-sectional study from Central India. *Indian Journal of Ophthalmology, 71*(5), 1905–1912. https://doi.org/10.4103/ijo.IJO_2020_22

Saul D, Kosinsky RL. Epigenetics of Aging and Aging-Associated Diseases. *International Journal of Molecular Sciences*. 2021; 22(1):401. https://doi.org/10.3390/ijms22010401

Scheid, R., Chen, J., & Zhong, X. (2021). Biological role and mechanism of chromatin readers in plants. *Current Opinion in Plant Biology*, *61*, 102008. https://doi.org/10.1016/j.pbi.2021.102008

Sedivy, J. M., Banumathy, G., & Adams, P. D. (2008). Aging by epigenetics--a consequence of chromatin damage?. *Experimental cell research, 314*(9), 1909–1917. https://doi.org/10.1016/j.yexcr.2008.02.023

Sen, P., Dang, W., Donahue, G., Dai, J., Dorsey, J., Cao, X., Liu, W., Cao, K., Perry, R., Lee, J. Y., Wasko, B. M., Carr, D. T., He, C., Robison, B., Wagner, J., Gregory, B. D., Kaeberlein, M., Kennedy, B. K., Boeke, J. D., & Berger, S. L. (2015). H3K36 methylation promotes longevity by enhancing transcriptional fidelity. *Genes & development, 29*(13), 1362–1376. https://doi.org/10.1101/gad.263707.115

Sen, P., Shah, P. P., Nativio, R., & Berger, S. L. (2016). Epigenetic Mechanisms of Longevity and Aging. *Cell, 166*(4), 822–839. https://doi.org/10.1016/j.cell.2016.07.050

Senner, C. E. (2011). The role of DNA methylation in mammalian development. *Reproductive BioMedicine Online, 22*(6), 529-535. Elsevier Ltd. https://doi.org/10.1016/j.rbmo.2011.02.016

Sharifi-Zarchi, A., Gerovska, D., Adachi, K., Totonchi, M., Pezeshk, H., Taft, R. J., Schöler, H. R., Chitsaz, H., Sadeghi, M., Baharvand, H., & Araúzo-Bravo, M. J. (2017). DNA methylation regulates discrimination of enhancers from promoters through a H3K4me1-H3K4me3 seesaw mechanism. *BMC Genomics, 18*(1). https://doi.org/10.1186/s12864-017-4353-7

Sidoli, S., Cheng, L., & Jensen, O. N. (2012). Proteomics in chromatin biology and epigenetics: Elucidation of post-translational modifications of histone proteins by mass spectrometry. *Journal of proteomics, 75*(12), 3419–3433. https://doi.org/10.1016/j.jprot.2011.12.029

Silverman, R. H. (2007). Viral Encounters with 2′,5′-Oligoadenylate Synthetase and RNase L during the Interferon Antiviral Response. *Journal of Virology*, 81(23), 12720–12729. https://doi.org/10.1128/jvi.01471-07

Sokolova, V., Sarkar, S., & Tan, D. (2023). Histone variants and chromatin structure, update of advances. *Computational and Structural Biotechnology Journal, 21*, 299–311. https://doi.org/10.1016/j.csbj.2022.12.002

Strahl, B. D., & Allis, C. D. (2000). The language of covalent histone modifications. *Nature, 403*(6765), 41–45. https://doi.org/10.1038/47412

Sweatt J. D. (2013). The emerging field of neuroepigenetics. *Neuron, 80*(3), 624–632. https://doi.org/10.1016/j.neuron.2013.10.023

Tan, K., & Wilkinson, M. F. (2023). Developmental regulators moonlighting as transposons defense factors. *Andrology, 11*(5), 891–903. https://doi.org/10.1111/andr.13427

Truong, T. P., Sakata-Yanagimoto, M., Yamada, M., Nagae, G., Enami, T., Nakamoto-Matsubara, R., Aburatani, H., & Chiba, S. (2015). Age-Dependent Decrease of DNA Hydroxymethylation in Human T Cells. *Journal of clinical and experimental hematopathology, 55*(1), 1–6. https://doi.org/10.3960/jslrt.55.1

Vaughan, R. M., Rothbart, S. B., & Dickson, B. M. (2019). The finger loop of the SRA domain in the E3 ligase UHRF1 is a regulator of ubiquitin targeting and is required for the maintenance of DNA methylation. *The Journal of biological chemistry, 294*(43), 15724–15732. https://doi.org/10.1074/jbc.RA119.010160

Wolffe, A. P., & Pruss, D. (1996). Hanging on to histones. Chromatin. *Current biology, 6*(3), 234–237. https://doi.org/10.1016/s0960-9822(02)00465-7

Wu, Z., Yang, M., Liu, H., Guo, H., Wang, Y., Cheng, H., & Chen, L. (2012). Role of nuclear receptor coactivator 3 (Ncoa3) in pluripotency maintenance. *The Journal of Biological Chemistry, 287*(45), 38295–38304. https://doi.org/10.1074/JBC.M112.373092

Xiao, C., Fan, T., Tian, H., Zheng, Y., Zhou, Z., Li, S., Li, C., & He, J. (2021). H3K36 trimethylation-mediated biological functions in cancer. *Clinical Epigenetics, 13*(1). BioMed Central Ltd. https://doi.org/10.1186/s13148-021-01187-2

Xie, B., Liu, Y., Zhao, Z., Liu, Q., Wang, X., Xie, Y., Liu, Y., Liu, Y., Yang, Y., Long, J., Dai, Q., & Li, H. (2020). MYB Proto-oncogene-like 1-TWIST1 Axis Promotes Growth and Metastasis of Hepatocellular Carcinoma Cells. *Molecular Therapy Oncolytics*, *18*, 58–69. https://doi.org/10.1016/j.omto.2020.05.016

Xie, Q., Zhao, S., Liu, W., Cui, Y., Li, F., Li, Z., Guo, T., Yu, W., Guo, W., Deng, W., & Gu, C. (2021). YBX1 Enhances Metastasis and Stemness by Transcriptionally Regulating MUC1 in Lung Adenocarcinoma. *Frontiers in oncology*, *11*, 702491. https://doi.org/10.3389/fonc.2021.702491

Xu, T., & Gao, H. (2020). Hydroxymethylation and tumors: Can 5-hydroxymethylation be used as a marker for tumor diagnosis and treatment? *Human Genomics, 14*(1), 15. BioMed Central Ltd. https://doi.org/10.1186/s40246-020-00265-5

Yi, S. J., & Kim, K. (2020). New Insights into the Role of Histone Changes in Aging. *International journal of molecular sciences, 21*(21), 8241. https://doi.org/10.3390/ijms21218241

Zhang, W., Qu, J., Liu, G. H., & Belmonte, J. C. I. (2020). The ageing epigenome and its rejuvenation. Nature reviews. *Molecular cell biology, 21*(3), 137–150. https://doi.org/10.1038/s41580-019-0204-5

Zhao, C., Yasui, K., Lee, C. J., Kurioka, H., Hosokawa, Y., Oka, T., & Inazawa, J. (2003). Elevated expression levels of NCOA3, TOP1, and TFAP2C in breast tumors as predictors of poor prognosis. *Cancer, 98*(1), 18–23. https://doi.org/10.1002/cncr.11482

Zhou, L., Shang, Y., Jin, Z., Zhang, W., Lv, C., Zhao, X., Liu, Y., Li, N., & Liang, J. (2015). UHRF1 promotes proliferation of gastric cancer via mediating tumor suppressor gene hypermethylation. *Cancer biology & therapy, 16*(8), 1241–1251. https://doi.org/10.1080/15384047.2015.1056411

Zhu, Q., Wang, D., Liang, F., Tong, X., Liang, Z., Wang, X., Chen, Y., & Mo, D. (2022). Protein arginine methyltransferase PRMT1 promotes adipogenesis by modulating transcription factors C/EBPβ and PPARγ. *The Journal of biological chemistry, 2 98*(9). https://doi.org/10.1016/j.jbc.2022.102309

Zuo, L., Prather, E. R., Stetskiv, M., Garrison, D. E., Meade, J. R., Peace, T. I., & Zhou, T. (2019). Inflammaging and oxidative stress in human diseases: From molecular mechanisms to novel treatments. *International Journal of Molecular Sciences*, *20*(18). MDPI AG. https://doi.org/10.3390/ijms20184472

Zhou, W., Liang, G., Molloy, P. L., & Jones, P. A. (2020). DNA methylation enables transposable element-driven genome expansion. *Proceedings of the National Academy of Sciences*, *117*(32), 19359-19366. https://doi.org/10.1073/pnas.1921719117